Modern Journal of Statistics
2(2), 81–102
DOI: https://doi.org/10.64389/mjs.2026.02283
https://sphinxsp.org/journal/index.php/mjs

Research article

A Novel Flexible Logarithmic Cosine-G Family of Distributions with Applications to Event Time Data

Zubir Shah[1,*], Zubair Ahmad[2], Zahra Almaspoor[2], Faridoon Khan[3], Chrisogonus K. Onyekwere[4], Gadde Srinivasa Rao[5], and Saima K. Khosa[6]

[1]Department of Statistics, Abdul Wali Khan University, Mardan, KP, 23200, Pakistan; Zubair_shah@awkum.edu.pk

[2]Department of Statistics, Yazd University, Yazd 8915818411, Iran; z.ferry21@gmail.com; zahra.ferry21@gmail.com

[3]Department of Creative Technologies, FCAI, Air University, Islamabad, Pakistan; faridoon.khan@au.edu.pk

[4]Nnamdi Azikiwe University, Awka, Nigeria; chrisogonusjohnson@gmail.com

[5]Department of Mathematics and Statistics, University of Dodoma, Dodoma P.O. Box 259, Tanzania; gadde.srinivasa@udom.ac.tz

[6]Department of Mathematics and Statistics, University of Saskatchewan, Saskatoon, SK S7N 5A2, Canada; skk807@mail.usask.ca

***Correspondence:** Zubair_shah@awkum.edu.pk.

ARTICLE INFO

Keywords:
Logarithmic Cosine-G
Estimation
Statistical properties
Simulation study
Biomedical data modeling

Mathematics Subject Classification:
62G05, 62H10, 62E15, 62N01

Important Dates:
Received: 18 April 2026
Revised: 16 May 2026
Accepted: 2 June 2026
Online: 4 June 2026

ABSTRACT

Many probability distributions have been developed in the literature on distribution theory to describe and forecast real-world phenomena, especially in the domains of engineering, sports, and medicine. To give the current distribution greater flexibility, these distributions are generated with the addition of one or more extra parameters. Reparameterization and estimation issues are the two major issues that arise when additional parameters are added to the existing distribution. We make a significant attempt to propose a novel statistical methodological strategy for generating more flexible distributions devoid of extra parameters to prevent the aforementioned two issues. The logarithmic and cosine functions are used to build the recently described approach. A Novel Flexible Logarithmic Cosine-G (NFLC-G) family of distributions is the name given to the newly suggested approach. Additionally, some distributional characteristics of the NFLC-G family are also obtained. Using the newly suggested approach, a unique sub-model known as the Novel Flexible Logarithmic Cosine Weibull (NFLC-Wei) distribution is established. The Maximum Likelihood estimation method is used to estimate the model parameters of the proposed family of distributions. Similarly, a comprehensive Monte Carlo simulation analysis verifies the accuracy of the parameter estimation technique. From simulation analysis, it is observed that as the sample size increases, the biases and mean square errors declined as well as MLEs gradually approach the true parameter values. Moreover, three sets of biomedical data are demonstrated to check the applicability of the NFLC-G family of distributions. Using statistical information criteria, the performance of the proposed distribution is compared to other well-known existing distributions. Finally, we found that the NFLC-Wei distribution appears to be the best option for the studied data sets based on these statistical information requirements.

1. Introduction

Research is the foundation of progress and the driving force of creativity. Given the importance of research in various applied science fields, many related studies have emerged. For example, [1] examined the hierarchical fuzzy topological framework for regression issues involving high-dimensional data. [2] examined the adaptive kernel regression-based test for conditional independence. [3] examined the research on promoting patient acceptance of online medical guidance via collaborative online consultations. [4] examined a zeroing neural network with time-varying fuzzy parameters for synchronizing chaotic systems. [5] concentrated on a flexible tempered reversible jump algorithm for Bayesian curve fitting.

In the statistical literature, researchers have produced several papers in the literature on distribution theory that suggest novel probability distributions for assessing and forecasting events in the real world, particularly in biomedical, engineering, actuarial, management, sports, and education sectors [6-9]. The Weibull (Wei) distribution is one of the most widely used probability distributions in the literature among these probability distributions [10-11]. Because of the Wei distribution's simple structure and straightforward cumulative distribution function (CDF) and probability density function (PDF), researchers have prioritized studying and forecasting real-world occurrences with this distribution, see Sarhan et al. [12]. When dealing with data that solely contains single-state failure rates, researchers have traditionally turned to the Wei distribution first. In fact, for the datasets that have single-state failure rates, the Wei distribution is the best choice in almost every field of life. On the other hand, for the datasets that have maxed-state failure rates, unfortunately, the Wei distribution does not afford the greatest fit for such situations; for further details, see Rehman et al. [13]. To prevail over this deficiency in the Wei and other existing distributions, a series of new methods for modification purposes has been considered and implemented. To get the upgraded version with increased distributional flexibility, these efforts have involved adding one or more extra parameters to the Wei or other existing distributions. The parameters of some of these updated versions have typically grown to seven or more; see Nofal et al. [14].

Kumar et al. [15] developed a new approach of probability distributions, called the SS transformation, by integrating a Sine trigonometric function with a baseline cumulative distribution function, the novel Sine-G family of probability distributions introduced by Mahmood et al. [16], another form of Sin-G class family of distributions proposed by Souza et al. [17], the Cos-G class family of distributions with real-life application introduced by Souza et al. [18], the Hyperbolic Tan-X family of probability distributions introduced by Ampadu et al. [19], the Teissier-G approach of probability distributions introduced by the authors Eghwerido et al. [20], and a unique probabilistic method for creating more flexible probability distributions introduced by Odhah et al. [21]. For more information about the families of probability distributions based on trigonometric functions, please see Ahmad et al. [22], Sapkota et al. [23], and Almetwally et al. [24].

Jiang et al. [25] recently introduced a new cosine-based approach for modeling time-to-event occurrences in the fields of engineering and sports. The CDF (cumulative distribution function) of their proposed family of distributions is given by

$$Y(w;\kappa) = cos\left(\frac{\pi}{2}\bar{G}(w;\kappa)\right)e^{1-cos\left(\frac{\pi}{2}\bar{G}(w;\kappa)\right)}, \qquad w \in \mathbb{R}, \qquad (1.1)$$

where, $\bar{G}(w;\kappa) = 1 - G(w;\kappa)$, and $\kappa$is the parameter vector of any baseline distribution. They used the Wei distribution as a baseline distribution and proposed a new distribution.

An alternative approach, known as the new Weighted Cosine-G Family of distributions, was also suggested by Odhah et al. [26]. Their suggested family of distributions' CDF is provided by

$$Y(w;\kappa) = \frac{e^{\left(1-cos\left(\frac{\pi G(w;\kappa)}{1+G(w;\kappa)}\right)\right)}-1}{e-1}, \qquad w \in \mathbb{R}, \qquad (1.2)$$

where, $G(w;\kappa)$is the CDF of any base distribution depending on the parameter vector κ.

Inspired by the thorough discussion above, we also proposed a new family of distributions in this study. Nowadays, trigonometric and logarithmic functions are commonly used to propose new approaches of probability distributions. The novel approach, which may be called the Novel Flexible Logarithmic Cosine-G (NFLC-G) family of distributions, is achieved without the need for extra parameters. Section 5 provides information on how the NFLC-G family of

distributions can increase the fitting power of the current (or existing) distributions.

Definition: Let $G(w;\kappa)$be the baseline CDF of any existing distribution with the corresponding PDF $g(w;\kappa)$; that is $\frac{d}{dw}G(w;\kappa) = g(w;\kappa)$. Then the CDF$Y(w;\kappa)$ of the NFLC-G family of probability distributions can be expressed as follows

$$Y(w;\kappa) = log\left(e + \left(1 - e^{cos\left(\frac{\pi}{2}G(w;\kappa)\right)}\right)\right), \qquad w \in \mathbb{R}. \tag{1.3}$$

The PDF of the NFLC-G family of distributions, say $y(w;\kappa)$is expressed as

$$y(w;\kappa) = \frac{d}{dw}Y(w;\kappa). \tag{1.4}$$

Using Eq. (1.3) in Eq. (1.4), we obtain

$$y(w;\kappa) = \frac{\pi g(w;\kappa)\, sin\left(\frac{\pi}{2}G(w;\kappa)\right)e^{cos\left(\frac{\pi}{2}G(w;\kappa)\right)}}{2\left(e+\left(1-e^{cos\left(\frac{\pi}{2}G(w;\kappa)\right)}\right)\right)}, \qquad w \in \mathbb{R}, \tag{1.5}$$

Where $g(w;\kappa) = \frac{d}{dw}G(w;\kappa)$.

As key reliability functions, the SF (survival or reliability function) $S(w;\kappa)$, HF (hazard function) $h(w;\kappa)$, and CHF (cumulative HF) $H(w;\kappa)$of the NFLC-G family of distributions are given by

$$S(w;\kappa) = 1 - log\left(e + \left(1 - e^{cos\left(\frac{\pi}{2}G(w;\kappa)\right)}\right)\right), \qquad w \in \mathbb{R}, \tag{1.6}$$

$$h(w;\kappa) = \frac{\pi g(w;\kappa)\, sin\left(\frac{\pi}{2}G(w;\kappa)\right)e^{cos\left(\frac{\pi}{2}G(w;\kappa)\right)}}{2\left(e+\left(1-e^{cos\left(\frac{\pi}{2}G(w;\kappa)\right)}\right)\right)\left(1-log\left(e+\left(1-e^{cos\left(\frac{\pi}{2}G(w;\kappa)\right)}\right)\right)\right)}, \qquad w \in \mathbb{R}, \tag{1.7}$$

and

$$H(w;\kappa) = -log\left(1 - log\left(e + \left(1 - e^{cos\left(\frac{\pi}{2}G(w;\kappa)\right)}\right)\right)\right), \qquad w \in \mathbb{R}, \tag{1.8}$$

respectively.

The next section of the article is based on the derivation of the New Flexible Logarithmic Cosine-Weibull (NFLC-Wei) distribution, which is a special sub-model of the proposed family of distributions. The Wei distribution is used as the foundational distribution in the NFLC-G family of distributions to present the NFLC-Wei distribution. The PDF$y(w;\kappa)$ and HF$h(w;\kappa)$ graphs of the NFLC-Wei distribution are also visualized in the same section. Section 3 discusses several distributional features of the NFLC-G family of distributions. In Section 4, the parameters of the NFLC-G distribution family are estimated utilizing the Maximum Likelihood Estimation (MLE) technique. Additionally, a Monte Carlo simulation analysis is conducted to evaluate the effectiveness of the MLE method in the same section. In Section 5, three real biomedical data sets are examined to evaluate the practical performance of the newly introduced distribution. Section 6 contains several concluding remarks.

2. NFLC-Wei Distribution

We derive the NFLC-Wei distribution by using $G(w;\kappa)$as the CDF of the Wei distribution is given by

$$G(w;\kappa) = 1 - e^{-\phi w^{\delta}}, \qquad \phi, \delta > 0, w \geq 0, \tag{2.1}$$

with PDF

$$g(w;\kappa) = \phi\delta w^{\delta-1}e^{-\phi w^{\delta}}, \qquad w > 0.$$

Subsequently, inserting Eq. (2.1) into Eq. (1.3), we obtain the revised form of the Wei distribution. The CDF of the NFLC-Wei distribution is expressed as:

$$Y(w;\kappa) = log\left(e + \left(1 - e^{cos\left(\frac{\pi}{2}\left(1-e^{-\phi w^{\delta}}\right)\right)}\right)\right), \qquad w \geq 0, \tag{2.2}$$

with the corresponding PDF$y(w;\kappa)$is

$$y(w;\kappa)=\frac{\pi\phi\delta w^{\delta-1}e^{-\phi w^{\delta}}\sin\left(\frac{\pi}{2}\left(1-e^{-\phi w^{\delta}}\right)\right)e^{\cos\left(\frac{\pi}{2}\left(1-e^{-\phi w^{\delta}}\right)\right)}}{2\left(e+\left(1-e^{\cos\left(\frac{\pi}{2}\left(1-e^{-\phi w^{\delta}}\right)\right)}\right)\right)},w>0. \quad (2.3)$$

Furthermore, link to Eq. (2.2) and Eq. (2.3), the SF $S(w;\kappa)$, HF $h(w;\kappa)$, CHF$H(w;\kappa)$of the NFLC-Wei distribution are presented as follows

$$S(w;\kappa)=1-log\left(e+\left(1-e^{\cos\left(\frac{\pi}{2}\left(1-e^{-\phi w^{\delta}}\right)\right)}\right)\right), \quad w>0, \quad (2.4)$$

$$h(w;\kappa)=\frac{\pi\phi\delta w^{\delta-1}e^{-\phi w^{\delta}}\sin\left(\frac{\pi}{2}\left(1-e^{-\phi w^{\delta}}\right)\right)e^{\cos\left(\frac{\pi}{2}\left(1-e^{-\phi w^{\delta}}\right)\right)}}{2\left(e+\left(1-e^{\cos\left(\frac{\pi}{2}\left(1-e^{-\phi w^{\delta}}\right)\right)}\right)\right)\left(1-log\left(e+\left(1-e^{\cos\left(\frac{\pi}{2}\left(1-e^{-\phi w^{\delta}}\right)\right)}\right)\right)\right)}, \quad (2.5)$$

and

$$H(w;\kappa)=-log\left(1-log\left(e+\left(1-e^{\cos\left(\frac{\pi}{2}\left(1-e^{-\phi w^{\delta}}\right)\right)}\right)\right)\right), \quad w>0, \quad (2.6)$$

respectively.

To display the applicability and flexibility of the NFLC-Wei distribution, some basic plots for the PDF $y(w;\kappa)$ ad HF$h(w;\kappa)$ are sketched in Figure 1. The PDF $y(w;\kappa)$ plots of the NFLC-Wei distribution capture different behaviors such as right skewed (green curve line), left skewed (black curve line), decreasing (blue line), and symmetrical (deep pink line).

Similarly, the plots of HF $h(w;\kappa)$ of NFLC-Wei distribution also capture different behaviors such as increasing (green and blue lines), decreasing (black line), uni-model (deep pink line), and increasing-decreasing-increasing (red line). These visual representations of the NFLC-Wei distribution evidently demonstrate that the functions exhibit a high level of flexibility (or adaptability).

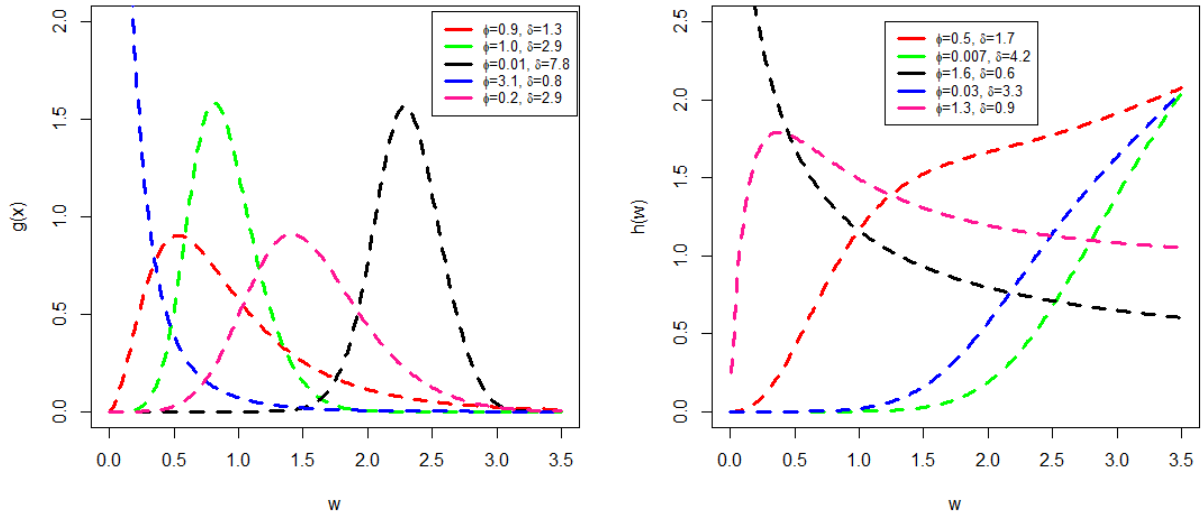

Figure 1. The graphical behavior of the PDF $y(w;\kappa)$ and HF$h(w;\kappa)$ of the NFLC-Wei distribution.

3. Statistical Properties

The statistical features of the NFLC-G family of distributions serve as the foundation for this section of the article. The statistical traits of the NFLC-G distributions consist of the quantile function, quartiles, skewness, kurtosis, moments, moment-generating function, and order statistics.

3.1. The quantile function

The QF (quantile function) of the NFLC-G family of probability distributions, say $Q(u)$is expressed by

$$Q(u) = G^{-1}\left(\frac{2}{\pi}cos^{-1}(log(e+1-e^{u}))\right), \quad (3.1)$$

where, $0 < u < 1$.

Since the mathematical formula in Equation (3.1) is in explicit form, it is straightforward to use it to generate random numbers from the NFLC-G distributions.

3.2. The quartile measures

The 1st quartile, 2nd quartile (commonly referred to as the median), and 3rd quartile of the NFLC-G family are obtained by substituting $u = \frac{1}{4}$, $u = \frac{1}{2}$, and $u = \frac{3}{4}$in Eq. (13), is expressed by

$$Q\left(\frac{1}{4}\right) = \frac{2}{\pi}G^{-1}\left(log\left(e+1-e^{\frac{1}{4}}\right)\right),$$

$$Q\left(\frac{1}{2}\right) = \frac{2}{\pi}G^{-1}\left(log\left(e+1-e^{\frac{1}{2}}\right)\right),$$

and

$$Q\left(\frac{3}{4}\right) = \frac{2}{\pi}G^{-1}\left(log\left(e+1-e^{\frac{3}{4}}\right)\right).$$

Furthermore, setting $u = 0.25$, $u = 0.75$, and the 25 and 75 percentiles are computed, respectively, in Eq. (3.1). The BOSK (Bowley's skewness) and MOKU (Moor's kurtosis) of the NFLC-G family are obtained.

3.3. The r^{th} moments

Let w be a random variable (RV) with a PDF $y(w;\kappa)$, then the r^{th}moments of the NFLC-G family of distributions, say $\mu_r^{'}$, is calculated as

$$\mu_r^{'} = E(W^r) = \int_{-\infty}^{\infty} w^r y(w;\kappa)dw. \quad (3.2)$$

Using Eq. (1.5) in Eq. (3.2), we calculate

$$\mu_r^{'} = \int_{-\infty}^{\infty} w^r \frac{\pi g(w;\kappa)\, sin\left(\frac{\pi}{2}G(w;\kappa)\right)e^{cos\left(\frac{\pi}{2}G(w;\kappa)\right)}}{2\left(e+\left(1-e^{cos\left(\frac{\pi}{2}G(w;\kappa)\right)}\right)\right)}dw,$$

$$\mu_r^{'} = \int_{-\infty}^{\infty} w^r \frac{\pi}{2e}g(w;\kappa)\, sin\left(\frac{\pi}{2}G(w;\kappa)\right)e^{cos\left(\frac{\pi}{2}G(w;\kappa)\right)}\left(1+e^{-1}\left(1-e^{cos\left(\frac{\pi}{2}G(w;\kappa)\right)}\right)\right)^{-1}dw. \quad (3.3)$$

As we know that

$$(1+w)^{-1} = \sum_{m=0}^{\infty}(-1)^m w^m. \quad (3.4)$$

Putting $w = e^{-1}\left(1-e^{cos\left(\frac{\pi}{2}G(w;\kappa)\right)}\right)$in Eq. (3.4), we derive

$$\left\{1-e^{-1}\left(1-e^{cos\left(\frac{\pi}{2}G(w;\kappa)\right)}\right)\right\}^{-1} = \sum_{m=0}^{\infty}(-1)^m e^{-m}\left(1-e^{cos\left(\frac{\pi}{2}G(w;\kappa)\right)}\right)^{m},$$

or

$$\left\{1-e^{-1}\left(1-e^{cos\left(\frac{\pi}{2}G(w;\kappa)\right)}\right)\right\}^{-1} = \sum_{m=0}^{\infty}\sum_{n=0}^{m}(-1)^{m+n}\binom{m}{n}e^{-m}e^{n\,cos\left(\frac{\pi}{2}G(w;\kappa)\right)}. \quad (3.5)$$

Using Eq. (3.5) in Eq. (3.3), we obtain

$$\mu_r^{'} = \sum_{m=0}^{\infty}\sum_{n=0}^{m}\frac{\pi}{2e}(-1)^{m+n}\binom{m}{n}e^{-(1+m)}\int_{-\infty}^{\infty} w^r g(w;\kappa)\, sin\left(\frac{\pi}{2}G(w;\kappa)\right)e^{(1+n)\,cos\left(\frac{\pi}{2}G(w;\kappa)\right)}dw. \quad (3.6)$$

As we also know that

$$e^{w} = \sum_{v=1}^{\infty}\frac{w^v}{v!}. \quad (3.7)$$

Using $w = (1+n)\,cos\left(\frac{\pi}{2}G(w;\kappa)\right)$in Eq. (3.7), we get

$$e^{(1+n)\cos\left(\frac{\pi}{2}G(w;\kappa)\right)} = \sum_{v=1}^{\infty} \frac{(1+n)^v \left(\cos\left(\frac{\pi}{2}G(w;\kappa)\right)\right)^v}{v!}. \quad (3.8)$$

By inserting Eq. (3.8) in Eq. (3.6), we obtain

$$\mu_r' = \sum_{m=0}^{\infty}\sum_{n=0}^{m}\sum_{v=1}^{\infty} \frac{\pi(1+n)^v}{2v!}(-1)^{m+n}\binom{m}{n} e^{-(1+m)} \int_{-\infty}^{\infty} w^r g(w;\kappa)\sin\left(\frac{\pi}{2}G(w;\kappa)\right) \times \left\{\sin\left(\frac{\pi}{2}G(w;\kappa)\right)\right\}^v dw,$$

$$\mu_r' = \sum_{m=0}^{\infty}\sum_{n=0}^{m}\sum_{v=1}^{\infty} \frac{\pi(1+n)^v}{2v!}(-1)^{m+n}\binom{m}{n} e^{-(1+m)} \Delta_{r,m,n,v}(w;\kappa), \quad (3.9)$$

where

$$\Delta_{r,m,n,v}(w;\kappa) = \int_{-\infty}^{\infty} w^r g(w;\kappa)\sin\left(\frac{\pi}{2}G(w;\kappa)\right)\left\{\cos\left(\frac{\pi}{2}G(w;\kappa)\right)\right\}^v dw.$$

Additionally, the Moment Generating (MG) function, say $M_w(t)$, of the NFLC-G family of distributions is calculated as

$$M_w(t) = \int_{-\infty}^{\infty} e^{wt} y(w;\kappa)dw \quad (3.10)$$

Using the exponential series $e^t = \sum_{r=1}^{\infty}\frac{t^r}{r!}$

$$M_w(t) = \sum_{r=1}^{\infty}\frac{t^r}{r!}\int_{-\infty}^{\infty} w^r y(w;\kappa)dw.$$

After simplification, we get the MG function

$$M_w(t) = \sum_{r=1}^{\infty}\sum_{m=0}^{\infty}\sum_{n=0}^{m}\sum_{v=1}^{\infty} \frac{t^r\pi(1+n)^v}{2v!r!}(-1)^{m+n}\binom{m}{n} e^{-(1+m)}\Delta_{r,m,n,v}(w;\kappa).$$

Setting r =1, 2, 3, and 4, respectively, in Eq. (3.9), some key measures (i.e., μ_1', μ_2', μ_3', μ_4', Variance, Skewness, and Kurtosis) of the NFLC-Wei to demonstrate the influence of the parameter values are presented in Table 1.

Table 1. The first four raw moments, skewness, and Kurtosis for different values $\phi$and δ.

Parameters		**Some key measures**						
ϕ	δ	μ_1'	μ_2'	μ_3'	μ_4'	Variance	Skewness	Kurtosis
0.3	0.7	5.88524	105.7164	3970.428	243581.9	71.08041	4.19109	33.34734
	1.4	2.05138	5.88524	22.27634	105.7164	1.67707	1.52999	6.54123
	2.1	1.55032	2.81697	5.88524	13.90574	0.41347	0.88766	4.11064
	2.8	1.36767	2.05138	3.34491	5.88524	0.18087	0.57941	3.44477
0.9	0.7	1.22507	4.58077	35.81228	457.3387	3.07996	4.19109	33.34734
	1.4	0.93593	1.22507	2.11564	4.58077	0.34909	1.52999	6.54123
	2.1	0.91879	0.98941	1.22507	1.71550	0.14523	0.88766	4.11063
	2.8	0.92380	0.93593	1.03082	1.22507	0.08252	0.57941	3.44477
2.7	0.7	0.25501	0.19849	0.32301	0.15867	0.13345	4.19109	33.34734
	1.4	0.42701	0.25501	0.20092	0.19848	0.07266	1.52998	6.54123
	2.1	0.54452	0.34752	0.25501	0.21163	0.05101	0.88766	4.11063
	2.8	0.62399	0.42701	0.31767	0.25501	0.03764	0.57957	3.44394

Table 1 shows that, for fixed values of ϕ, the first four raw moments, variance, Skewness, and Kurtosis of the NFLC-Wei distribution decrease as δincreases. Similarly, for the same values of parameters, the Skewness and Kurtosis values are also decreased. Furthermore, from Table 1, we can also see that the NFLC-Wei distribution shows positive skewness and a leptokurtic distribution as the skewness > 0 and kurtosis > 3. Hence, the proposed distribution is also more versatile and a good candidate for modeling positively skewed data sets.

3.4. Order statistic

Let $W_1, W_2, \ldots, W_p$ be the random sample of size p taken from the proposed NFLC-G family with their corresponding CDF $Y(w;\kappa)$and PDF $y(w;\kappa)$ presented in Eq. (1.3) and Eq. (1.5), respectively. Then the density function (DF) of pth

order statistics (OS) of the NFLC-G family, say$y_{r:p}(w)$, is presented by

$$y_{r:p}(w) = \frac{1}{B(r,p-r+1)} y(w;\kappa)[Y(w;\kappa)]^{r-1}[1-Y(w;\kappa)]^{p-r}. \quad (3.11)$$

The 1^{st} and p^{th} OS can be expressed as $W_{1:p} = min(W_1, W_2, \ldots, W_p)$and $W_{p:p} = max(W_1, W_2, \ldots, W_p)$since for$w > 0$the CDF of the NFLC-G family follows the $0 < Y(w;\kappa) < 1$. Now, by utilizing the binomial expansion of $[1-Y(w;\kappa)]^{p-r}$as follow

$$[1-Y(w;\kappa)]^{p-r} = \sum_{i=0}^{p-r}(-1)^i [Y(w;\kappa)]^i. \quad (3.12)$$

By inserting Eq. (3.12) into Eq. (3.11), then, we get

$$y_{r:p}(w) = \frac{y(w;\kappa)}{B(r,p-r+1)} \sum_{i=0}^{p-r}(-1)^i [Y(w;\kappa)]^{r+i-1}. \quad (3.13)$$

Applying Eq. (1.3) and Eq. (1.5) in Eq. (3.13), we can obtain the DF of $y_{r:p}(w)$.

4. Estimation and Simulation

There are two subsections in this section of the article. The NFLC-G family of distributions' estimators of the parameters (ϕ, δ) are derived in the first subsection using maximum likelihood estimation, or MLE$(\hat{\phi}_{MLE}, \hat{\delta}_{MLE})$. In contrast, the second subsection uses simulation analysis to assess how well the MLEs$(\hat{\phi}_{MLE}, \hat{\delta}_{MLE})$ of the NFLC-Wei distribution's parameters(ϕ, δ) perform (both numerically and visually).

4.1. Estimation

Let $W_1, W_2, W_3, \ldots . W_n$ be the RS (random sample) of size m taken from the NFLC-Wei distribution with PDF $y(w;\kappa)$, then the likelihood function (LHF) corresponding to the PDF is given by

$$\gamma(w) = \prod_{i=1}^{m} y(w;\kappa). \quad (4.1)$$

Using PDF $y(w;\kappa)$of Eq. (2.3) in Eq. (4.1), we get

$$\gamma(w) = \prod_{i=1}^{m} \frac{\pi\phi\delta w^{\delta-1} e^{-\phi w^{\delta}} \sin\left(\frac{\pi}{2}\left(1-e^{-\phi w^{\delta}}\right)\right) e^{\cos\left(\frac{\pi}{2}\left(1-e^{-\phi w^{\delta}}\right)\right)}}{2\left(e+\left(1-e^{\cos\left(\frac{\pi}{2}\left(1-e^{-\phi w^{\delta}}\right)\right)}\right)\right)}.$$

The log LHF (LLHF), say$\ell(\phi, \delta)$, is given by

$$\ell(\phi,\delta) = m\log\left(\frac{\pi}{2}\right) + m\log\phi + m\log\delta + (\delta-1)\sum_{i=1}^{m}\log w_i + \sum_{i=1}^{n}\cos\left(\frac{\pi}{2}\left(1-e^{-\phi w^{\delta}}\right)\right)$$
$$+\sum_{i=1}^{n}\log\sin\left(\frac{\pi}{2}\left(1-e^{-\phi w^{\delta}}\right)\right) - \sum_{i=1}^{n}\log\left[e^{\phi}+\left(1-e^{\cos\left(\frac{\pi}{2}\left(1-e^{-\phi w^{\delta}}\right)\right)}\right)\right] \quad . \quad (4.2)$$

Corresponding to $\ell(\phi, \delta)$, the partial derivatives determined by ϕ and δ are as follows:

$$\frac{d}{d\phi}\ell(\phi,\delta) = \frac{m}{\phi} - \frac{\pi}{2}\sum_{i=1}^{m}\sin\left(\frac{\pi}{2}\left(1-e^{-\phi w_i{}^{\delta}}\right)\right) w^{\delta} e^{-\phi w_i{}^{\delta}} + \frac{\pi}{2}\sum_{i=1}^{m}\frac{\cos\left(\frac{\pi}{2}\left(1-e^{-\phi w_i{}^{\delta}}\right)\right) w^{\delta} e^{-\phi w_i{}^{\delta}}}{\sin\left(\frac{\pi}{2}\left(1-e^{-\phi w_i{}^{\delta}}\right)\right)}$$
$$-\frac{\pi}{2}\sum_{i=1}^{m}\frac{\sin\left(\frac{\pi}{2}\left(1-e^{-\phi w_i{}^{\delta}}\right)\right) e^{\cos\left(\frac{\pi}{2}\left(1-e^{-\phi w_i{}^{\delta}}\right)\right)} w^{\delta} e^{-\phi w_i{}^{\delta}}}{\left[e+\left(1-e^{\cos\left(\frac{\pi}{2}\left(1-e^{-\phi w_i{}^{\delta}}\right)\right)}\right)\right]},$$

and

$$\frac{d}{d\delta}\ell(\phi,\delta)=\frac{m}{\delta}+log\,w_i+\frac{\pi\phi}{2}\sum_{i=1}^{m}\frac{cos\left(\frac{\pi}{2}\left(1-e^{-\phi w_i{}^{\delta}}\right)\right)(log\,w_i)w_i{}^{\delta}e^{-\phi w_i{}^{\delta}}}{sin\left(\frac{\pi}{2}\left(1-e^{-\phi w_i{}^{\delta}}\right)\right)}$$

$$-\frac{\pi\phi}{2}\sum_{i=1}^{m}\frac{(log\,w_i)w_i{}^{\delta}e^{-\phi w_i{}^{\delta}}\,sin\left(\frac{\pi}{2}\left(1-e^{-\phi w_i{}^{\delta}}\right)\right)e^{cos\left(\frac{\pi}{2}\left(1-e^{-\phi w_i{}^{\delta}}\right)\right)}}{\left[e+\left(1-e^{cos\left(\frac{\pi}{2}\left(1-e^{-\phi w_i{}^{\delta}}\right)\right)}\right)\right]}$$

$$-\frac{\pi\phi}{2}\sum_{i=1}^{m}sin\left(\frac{\pi}{2}\left(1-e^{-\phi w_i{}^{\delta}}\right)\right)(log\,w_i)w^{\delta}e^{-\phi w_i{}^{\delta}},$$

Solving numerically $\frac{d}{d\phi}\ell(\phi,\delta)=0$, and $\frac{d}{d\delta}\ell(\phi,\delta)=0$, simultaneously, we get MLEs $(\hat{\phi}_{MLE},\hat{\delta}_{MLE})$ of the (ϕ,δ) of the NFLC-Wei distribution. As we can see that the equations i.e., $\frac{d}{d\phi}\ell(\phi,\delta)$, and $\frac{d}{d\delta}\ell(\phi,\delta)$have no closed form.

4.2. Simulation

In this sub-section, we evaluate the behaviors of the MLEs $(\hat{\phi}_{MLE},\hat{\delta}_{MLE})$ estimated by the MLE method. The MCSS (Monte Carlo simulation study) is used for evaluation purposes. The MCSS of the NFLC-Wei distribution is conducted for the four combinations of the values of the parameters ϕ and δ. The sets of parameter combinations are Set I = {ϕ =0.8, δ =1.7}, Set II= {ϕ =1.0, δ =1.8}, Set III= {ϕ =2.3, δ =1.9}, and Set IV= {ϕ =1.0, δ =1.3}. In general, there are no restrictions on the selection of the initial parameter values when conducting a simulation analysis. As we have already discussed, the range of parameter values of the proposed distributions is $\phi(\phi>0)$, and$\delta(\delta>0)$. Hence, we can choose any parameter values lying within these ranges for the simulation analysis. The values for the estimator are gathered from various sample sizes derived from the NFLC-Wei distribution; these sizes include 25, 50, 100, 200, 300, 400, 500, 600, 700, 800, 900, and 1000. For every sample size, the simulation study (or entire procedure) is conducted 1000 times. To check the performance of $(\hat{\phi}_{MLE},\hat{\delta}_{MLE})$for the newly NFLC-Wei distribution, we analyze three statistical measures, such as (i) biases and (ii) MSEs (mean square errors), utilizing the R language software. The corresponding mathematical representations are provided by

$$Bias(\hat{\theta}_{MLE})=\frac{1}{1000}\sum_{i=1}^{1000}(\hat{\theta}_i-\Theta),$$

and

$$MSE(\hat{\theta}_{MLE})=\frac{1}{1000}\sum_{i=1}^{1000}(\hat{\theta}_i-\Theta)^2,$$

where, $\Theta=(\phi,\delta)$.

Corresponding to Set I= {ϕ =0.8, δ =1.7}, Set II= {ϕ =1.0, δ =1.8}, Set III= {ϕ =2.3, δ =1.9}, and Set IV= {ϕ =1.0, δ =1.3}, the numerical results are recorded in Tables 2 and 3 (for numerical illustrations) and visualized in Figures 2-4 (for graphical illustrations). Based on numerical illustration (reported in Tables 2 and 3) and graphical illustration (visualized in Figures 2-4), we can clearly see that as the sample size rises (i.e., $n\to\infty$), then

- The estimated values$\hat{\phi}_{MLE}$and $\hat{\delta}_{MLE}$approaches the true values,
- The MSE values of $\hat{\phi}_{MLE}$and $\hat{\delta}_{MLE}$ approaches zero,
- The $\hat{\phi}_{MLE}$ and $\hat{\delta}_{MLE}$ Biases gradually decline.

Table 2. The MCSS results for NFLC-Wei distribution with different combinations of parameter values

n	Parameters	Set I: ϕ =0.8, δ =1.7			Set II: ϕ =1.0, δ =1.8		
		MLE	MSE	Bias	MLE	MSE	Bias
25	ϕ	0.830202	0.027044	0.030203	1.032790	0.048265	0.032791
	δ	1.802337	0.099332	0.102337	1.902436	0.100124	0.102436
75	ϕ	0.812221	0.010923	0.012222	1.019350	0.010788	0.009195
	δ	1.749487	0.038285	0.049487	1.850468	0.027245	0.038970
	ϕ	0.804831	0.004890	0.007986	1.009195	0.008329	0.008417

100	δ	1.716367	0.015565	0.030677	1.838970	0.018094	0.022466
200	ϕ	0.805146	0.002405	0.004831	1.003663	0.003926	0.006471
	δ	1.713370	0.007841	0.016366	1.810488	0.008953	0.019377
300	ϕ	0.802083	0.001595	0.004146	1.003677	0.002855	0.005405
	δ	1.704792	0.004981	0.013369	1.810089	0.006258	0.010698
400	ϕ	0.800878	0.001345	0.002083	1.003635	0.001764	0.003327
	δ	1.707112	0.003812	0.004792	1.807568	0.004864	0.005081
500	ϕ	0.801732	0.000909	0.000878	1.001777	0.001557	0.001776
	δ	1.702673	0.002935	0.007112	1.806050	0.003678	0.006050
600	ϕ	0.799547	0.000802	0.000173	1.001099	0.001220	0.001099
	δ	1.703327	0.002612	0.002673	1.805689	0.002841	0.005689
700	ϕ	0.801914	0.000674	0.000131	1.000708	0.001137	0.000708
	δ	1.704631	0.002269	0.002654	1.801126	0.002504	0.003126
800	ϕ	0.799813	0.000575	0.000106	1.001626	0.000954	0.000162
	δ	1.701854	0.001852	0.001841	1.803622	0.002188	0.002235
900	ϕ	0.800705	0.000548	0.000086	1.001391	0.000888	0.000159
	δ	1.700876	0.001657	0.001534	1.803385	0.001887	0.001967
1000	ϕ	0.800416	0.000474	0.000026	1.000237	0.000754	0.000137
	δ	1.703276	0.001544	0.001134	1.802453	0.001691	0.001452

Table 3. The MCSS results for NFLC-Wei distribution with different combinations of parameter values

		Set III: ϕ =2.3, δ =1.9			Set IV: ϕ =1.0, δ =1.3		
n	Parameters	MLE	MSE	Bias	MLE	MSE	Bias
25	ϕ	2.554453	0.553892	0.254453	1.043814	0.054966	0.043814
	δ	2.019893	0.115111	0.119893	1.372429	0.053080	0.072428
75	ϕ	2.375672	0.110953	0.075672	1.013782	0.010731	0.013782
	δ	1.937922	0.028924	0.037922	1.320321	0.013339	0.020320
100	ϕ	2.371203	0.081964	0.071203	1.006145	0.007596	0.006145
	δ	1.935302	0.020413	0.035302	1.316948	0.009947	0.016948
200	ϕ	2.332030	0.035770	0.032029	1.002801	0.003610	0.002801
	δ	1.917793	0.010015	0.017792	1.310282	0.004562	0.010281
300	ϕ	2.315114	0.023096	0.015113	1.003933	0.002826	0.003933
	δ	1.908753	0.006568	0.008753	1.305751	0.003124	0.005751
400	ϕ	2.312634	0.016895	0.012633	1.003192	0.001789	0.003193
	δ	1.906230	0.004584	0.006229	1.303897	0.002334	0.003896
	ϕ	2.312317	0.013218	0.012316	1.002462	0.001424	0.001712

500	δ	1.908615	0.003876	0.005615	1.304587	0.001754	0.003071
600	ϕ	2.315069	0.011914	0.011068	1.000603	0.001162	0.001266
	δ	1.902202	0.003301	0.005402	1.303527	0.001556	0.002029
700	ϕ	2.303360	0.009401	0.001065	1.001954	0.001169	0.001154
	δ	1.903883	0.002787	0.002183	1.303039	0.001234	0.001838
800	ϕ	2.304760	0.008375	0.001060	1.000323	0.000938	0.000323
	δ	1.904568	0.002379	0.002068	1.300820	0.001088	0.000820
900	ϕ	2.301030	0.007324	0.000929	1.001413	0.000834	0.000128
	δ	1.900076	0.002052	0.000761	1.301721	0.000942	0.000661
1000	ϕ	2.311168	0.007085	0.000116	1.001037	0.000716	0.000105
	δ	1.905048	0.001933	0.005048	1.301486	0.000895	0.000423

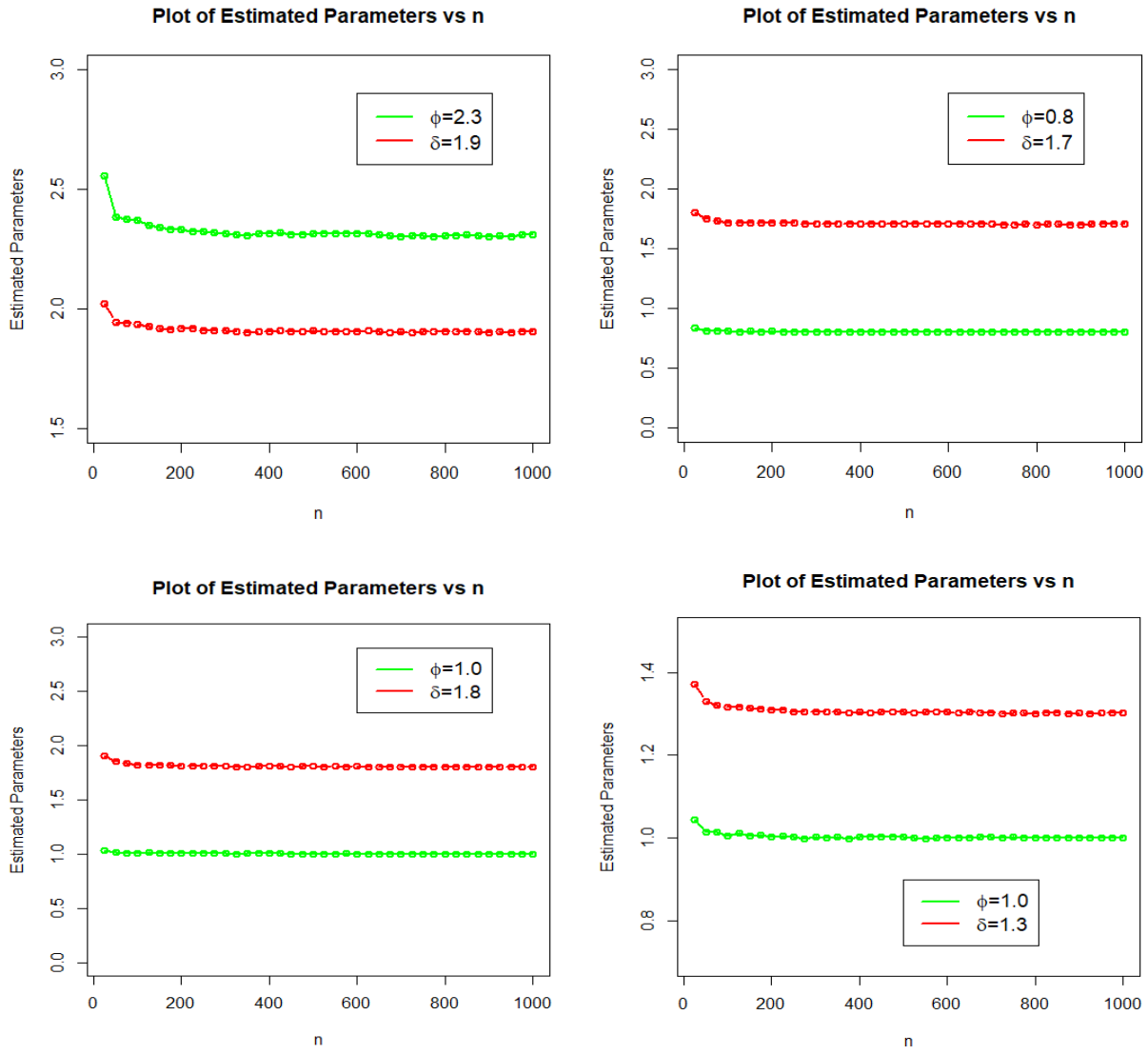

Figure 2. Visual (or graphical) illustration of MLEs of NFLC-Wei distribution for Sets I-IV.

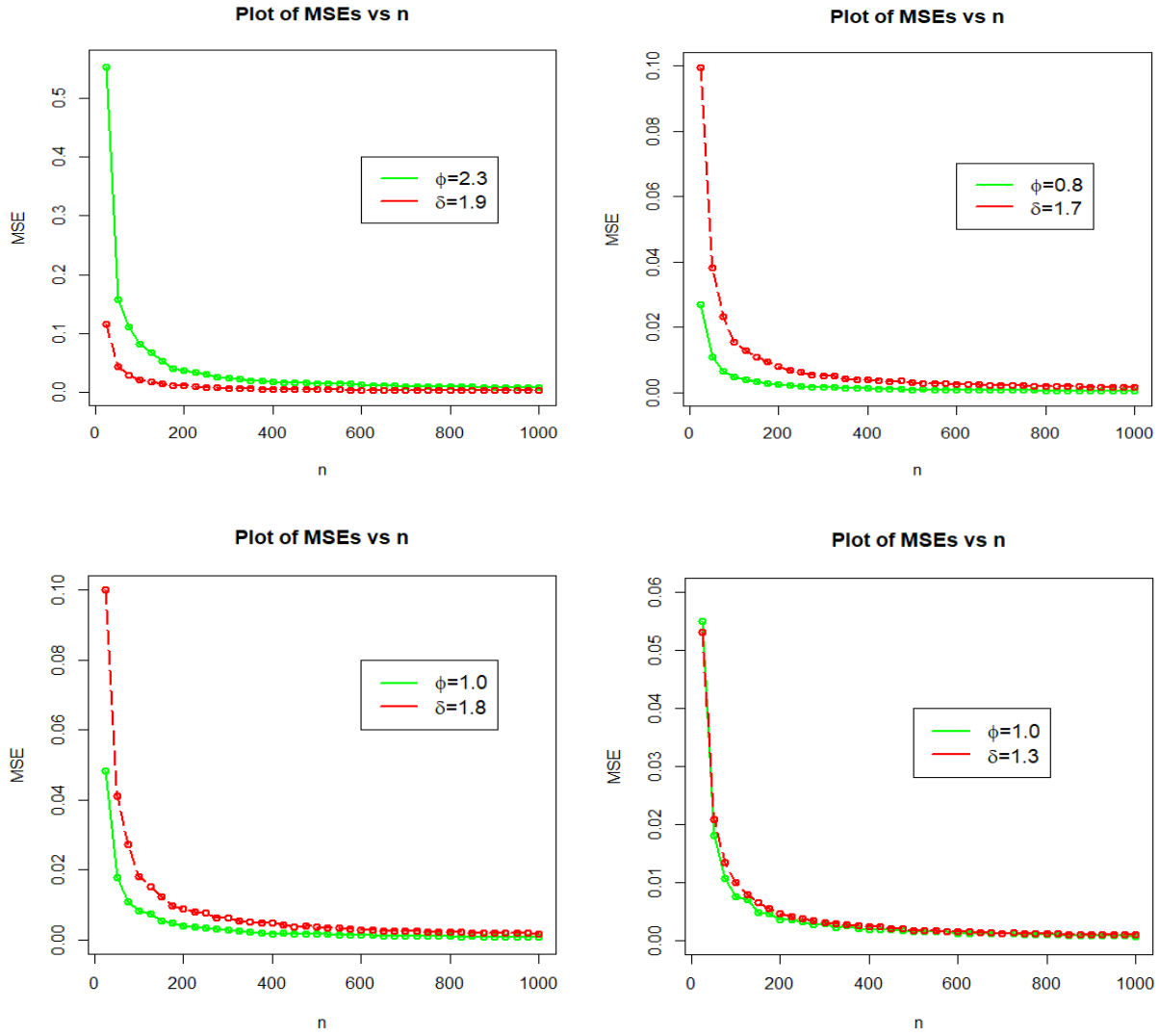

Figure 3. Visual (or graphical) illustration of MSEs of NFLC-Wei distribution for Sets I-IV.

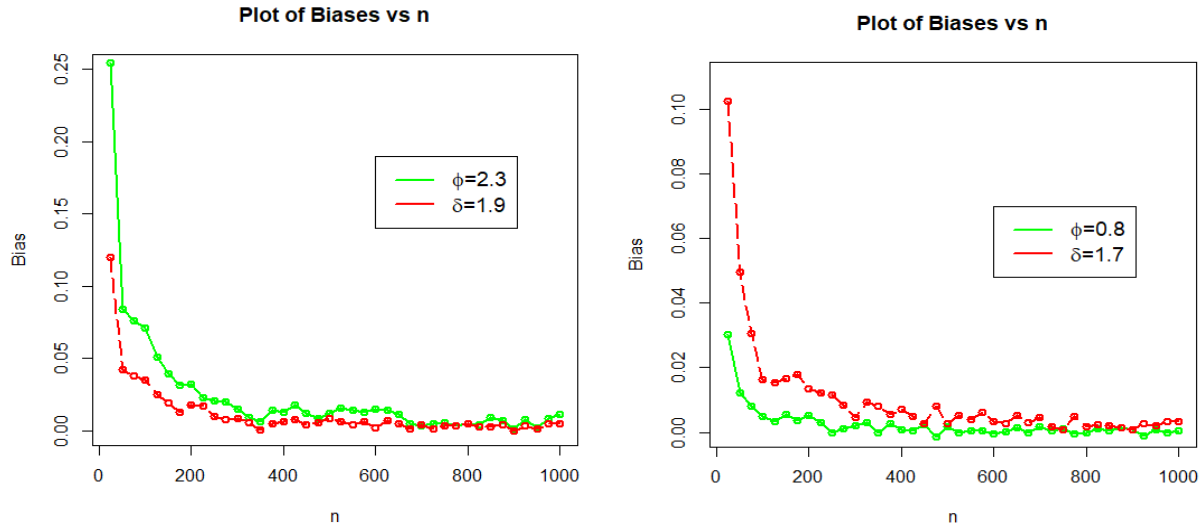

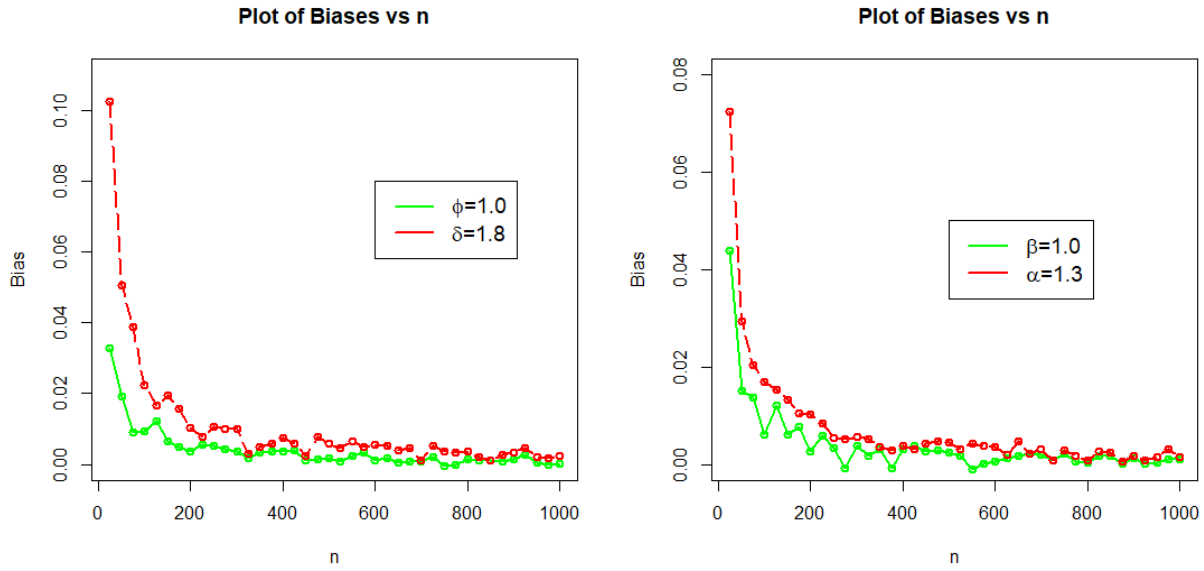

Figure 4. Visual (or graphical) illustration of Biases of the NFLC-Wei distribution for Sets I-IV.

5. Application of the NFLC-Wei Distribution

This section of the paper examines three real-world data sets from the biomedical industry, and it compares the NFLC-Wei distribution's goodness measures that is, best-fitting power with those of other rival (or competing) distributions, including new exponential Weibull (for short, NEx-Wei) of Shah et al. [27], the traditional Weibull distribution (for short, Wei) of Weibull [28], alpha power Cosine Weibull (for short, APC-Wei) of the authors of Alghamdi et al. [29], alpha Power Transform Weibull (for short, APT-Wei) of the researchers of Dey et al. [30], new APT-Wei (for short, NAPT-Wei) of Elbatal et al. [31], the Marshal Olkin Weibull distribution (for short, MO-Wei) of Marshal Olkin [32], and the new reduced logarithmic Weibull (for short, NRLog-Wei) proposed by the authors Liu et al. [33]. The goodness of fit measures consist of seven information criteria (IC) including Akiak IC (for short, AIC and onward, is expressed by Δ_1), Bayesian IC (for short, BIC and onward, this is expressed by Δ_2), Hannan Quinn IC (for short, HQIC and onward, this IC is expressed by Δ_3), Consistent AIC (for short, CAIC and onward, this IC is expressed by Δ_4), Kolmogorov-Smirnov (for short, KS and onward this IC onward is expressed by Δ_5), Anderson–Darling (for short, AD and onward this IC is expressed by Δ_6), Cramer-von-Misses (for short, CM and onward this IC is expressed by Δ_7), and its P-Values. Generally, the best-suited (superior fit to Data 1, Data 2, and Data 3) distribution will be a distribution whose least values of goodness measures (i.e., Δ_1, Δ_2, Δ_3, Δ_4, Δ_5, Δ_6, andΔ_7) and a higher P value.

5.1. Description of the biomedical data sets

The first medical data set (onward, the data set is represented by D_1) represents the patient's remission times (suffering from bladder cancer) totaling about 128 observations. The data set was originally reported by Lee et al. [34]. Some descriptive measures (i.e., summary measures) of D_1 are outlined as: minimum (D_1) = 0.080, maximum (D_1) = 79.050, Q1 (D_1) = 3.348, median (D_1) = 6.395, Q3 (D_1) = 11.838, mean (D_1) = 9.366, variance (D_1) = 110.425, rang (D_1) =78.97, skewness (D_1) =3.286569, and kurtosis (D_1) =18.48308.

The lifetimes of 20 patients on analgesics are reflected in the second medical data set (ahead, the data set is represented by D_2). A more recent study based on D_2, we refer to Lee et al. [34] and Shah et al. [35]. Some descriptive measures (i.e., summary measures) of D_2 are outlined as: minimum (D_2) = 1.100, maximum (D_2) =4.100, Q1 (D_2) =1.475, median (D_2) =1.700, Q3 (D_2) =2.050, mean (D_2) =1.900, variance (D_2) =0.4957895, rang (D_2) =3.0, skewness (D_2) =1.71975, and kurtosis (D_2) =5.924108.

The third set of biomedical data (ahead, the data set is represented byD_3) illustrates the survival duration of guinea pigs exposed to different levels of virulent tubercle bacilli. It consists of 72 observations. A more recent study aboutD_3, we refer to Shah et al. [36] and Odhah et al. [37]. Some descriptive measures (i.e., summary measures) of D_3 are outlined as: minimum (D_3) =12.20, maximum (D_3) =1776.00, Q1 (D_3) =67.21, median (D_3) =128.50, Q3 (D_3) =219.00, mean (D_3) =223.48, variance (D_3) =93286.41, rang (D_3) =1763.8, skewness (D_3) =3.38382, and kurtosis (D_3) =16.5596.

Additionally, linked toD_1,D_2, and D_3, some basic descriptive plots, respectively are visualized in Figures 5, 6, and 7.

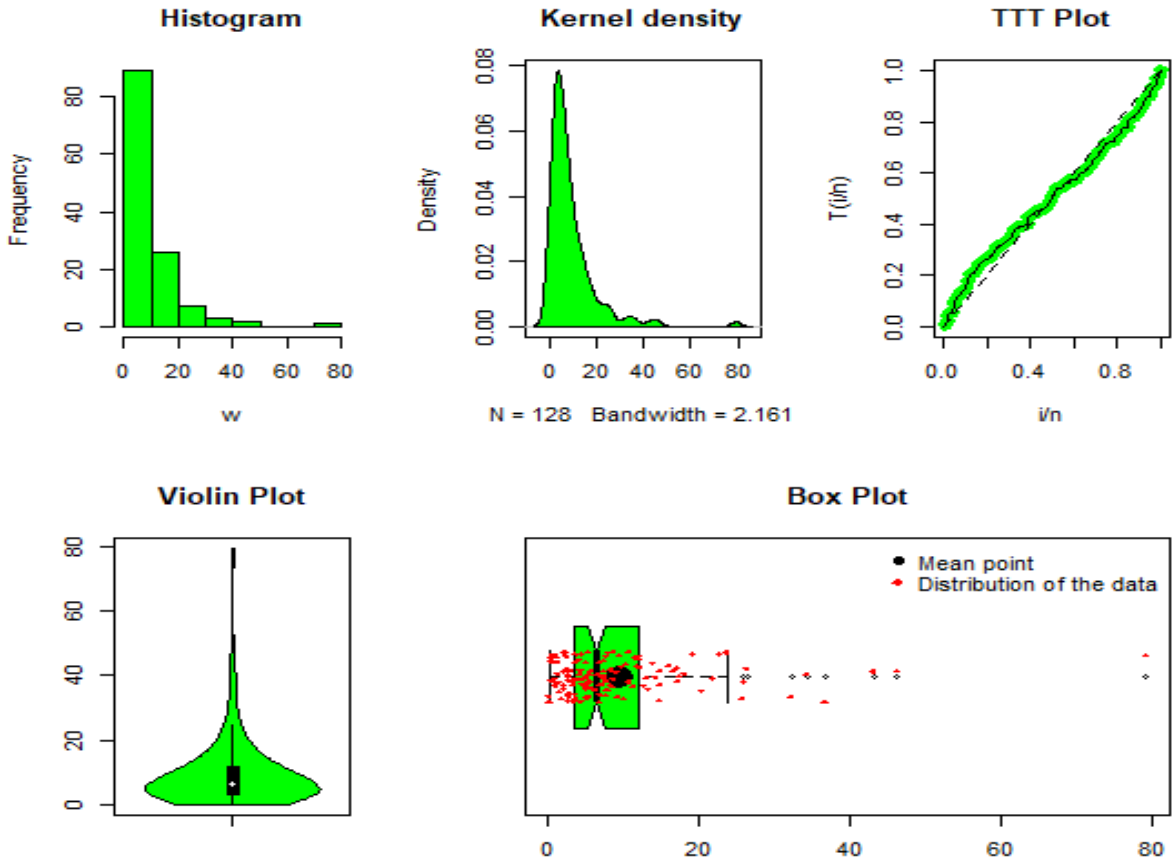

Figure 5. Some key plots for the D_1.

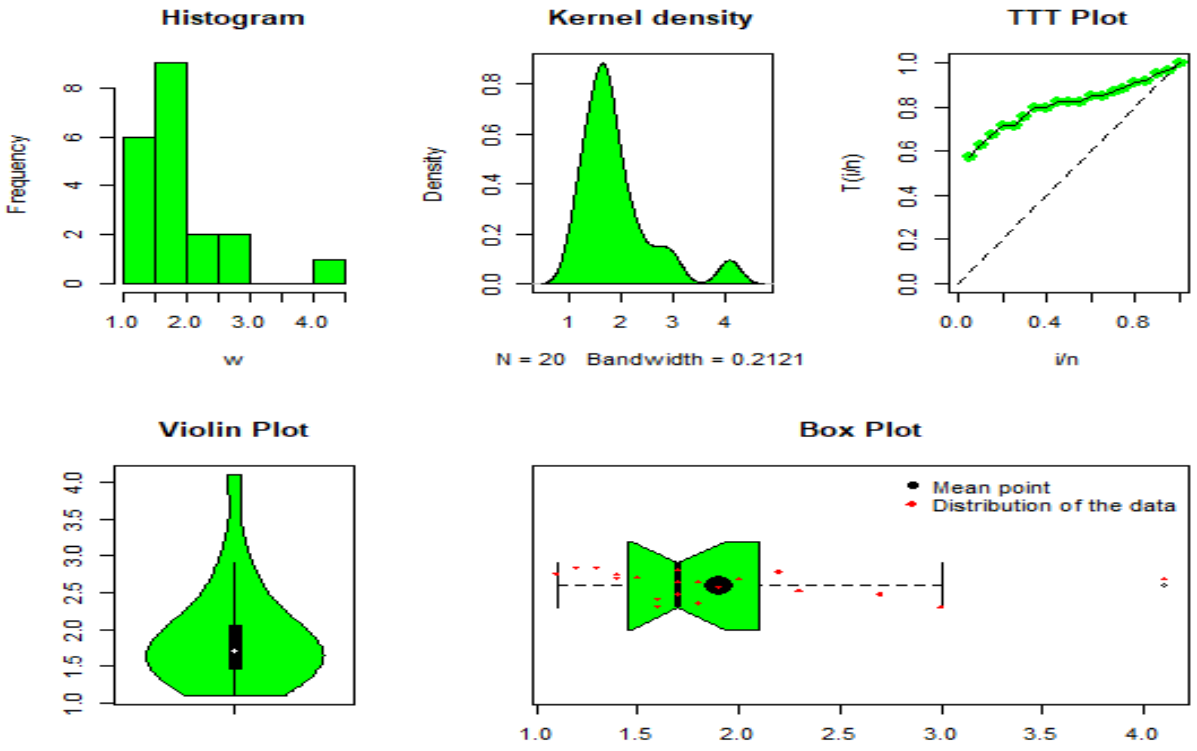

Figure 6. Certain basic plots for the D_2.

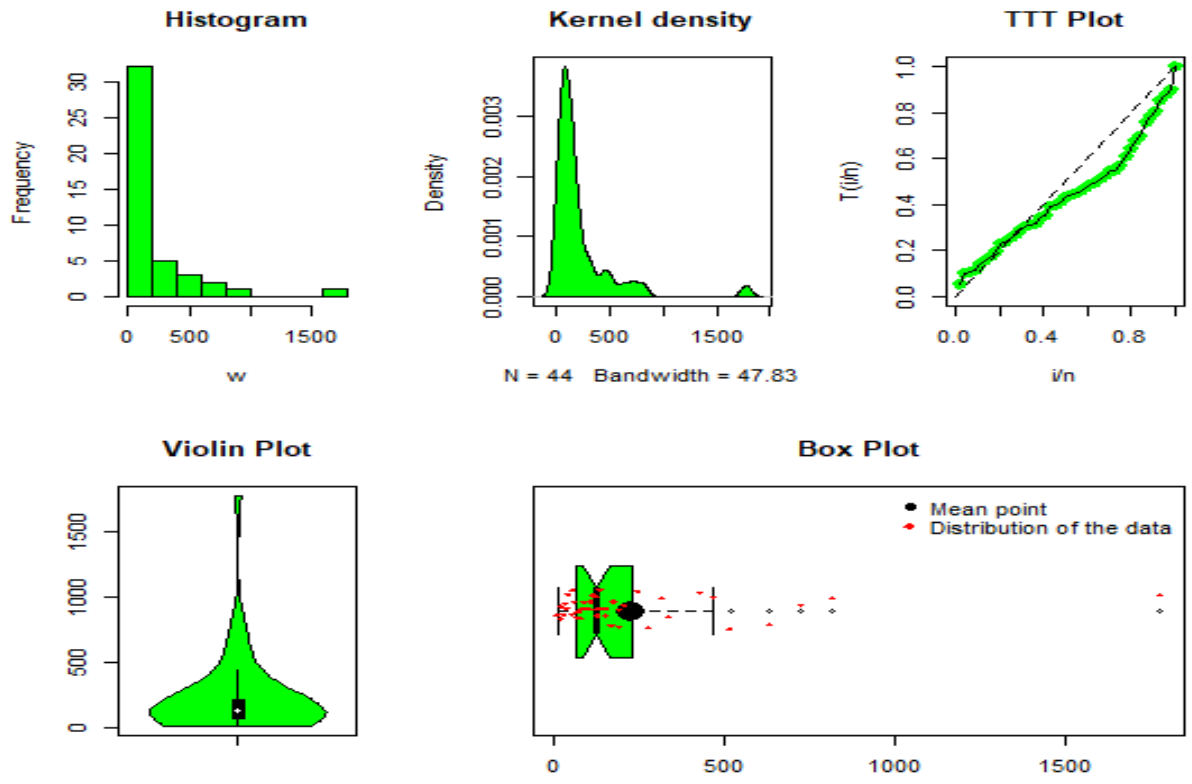

Figure 7. The key summary plots of the D_3.

5.2. Analysis of D_1

This sub-section of the article provides the numerical results of the MLEs and goodness of fit measures of the NFLC-Wei and other rival distributions usingD_1. The graphical illustrations of the fitting power of the NFLC-Wei distribution are also visualized using D_1.

Using D_1, the numerical values of the $\hat{\phi}_{MLE}$, $\hat{\alpha}_{MLE}$, and $\hat{\delta}_{MLE}$of the NFLC-Wei distribution and other competing (or rival) distributions are recorded in Table 4. The profile LLF of the $\hat{\phi}_{MLE}$ and $\hat{\delta}_{MLE}$of the NFLC-Wei distribution is graphically visualized in Figure 8. From Figure 8, we can see that the estimated parameters are unique roots and maximization of the LLF of the NFLC-Wei distribution.

Corresponding to D_1, the numerical descriptions of the goodness measures and p-values of the NFLC-Wei and other competing probability distributions are recorded in Table 5. From Table 5, for the NFLC-Wei distribution, the goodness of fit measures (or IC) and their P-value are: Δ_1 =824.9195, Δ_2 =830.6235, Δ_3 =825.0155, Δ_4 =827.2371, Δ_5 =0.035680, Δ_6 =0.25255, Δ_7 =0.03636, and P-value=0.9968. Based on the results of Δ_1, Δ_2, Δ_3, Δ_4, Δ_5, Δ_6, Δ_7, and P-value in Table 5, it is concluded that the NFLC-Wei probability distribution affords the superior and closed fits to the D_1. Because in Table 5, the NFLC-Wei distribution secures the smaller values of the goodness measures (i.e., Δ_1, Δ_2, Δ_3, Δ_4, Δ_5, Δ_6, and Δ_7) and a higher P-value. Furthermore, based on the results of Δ_1, Δ_2, Δ_4, Δ_5, Δ_6, Δ_7, and P-value recorded in Table 5, the second optimal distribution for theD_1 is the NAPT-Wei distribution. For the NAPT-Wei distribution, the goodness of fit measures and P-value are Δ_1 =826.1121, Δ_2 =834.6682, Δ_4 =828.3056, Δ_5 =0.042005, Δ_6 =0.2743269, Δ_7 =0.031732, and P-value=0.9776. Similarly, based on the results of the Δ_3, the second most optimal probability distributions for the D_1 is the APT-Wei distribution because its value is Δ_3 =826.5737.

After the numerical comparison, we also considered the graphical illustration of the NFLC-Wei distribution by usingD_1. For graphical illustrations, we visualized the plots of the estimated PDF, CDF, SF, and QQ plot, see Figure 9. The visual illustration in Figure 9 also confirmed that the NFLC-Wei distribution is a superior distribution for the D_1.

Table 4. The $\hat{\delta}_{MLE}$,$\hat{\alpha}_{1MLE}$, and $\hat{\alpha}_{2MLE}$ values of the NFLC-Wei and other rival distributions for D_1.

Dist.	$\hat{\phi}_{MLE}$	$\hat{\delta}_{MLE}$	$\hat{\alpha}_{MLE}$
NFLC-Wei	0.13501160	0.86781290	--
NRLog-Wei	0.03130656	1.27918190	0.81868158
Wei	0.09394292	1.04763386	--
APC-Wei	0.01225151	1.22089081	0.0225186 2
APT-Wei	0.01661290	1.26652923	0.01490768
NEx-Wei	0.03637109	1.21679224	--
NAPT-Wei	0.69708860	0.57210631	61.5874856
MO-Wei	2.39646531	0.35745640	105.7400692

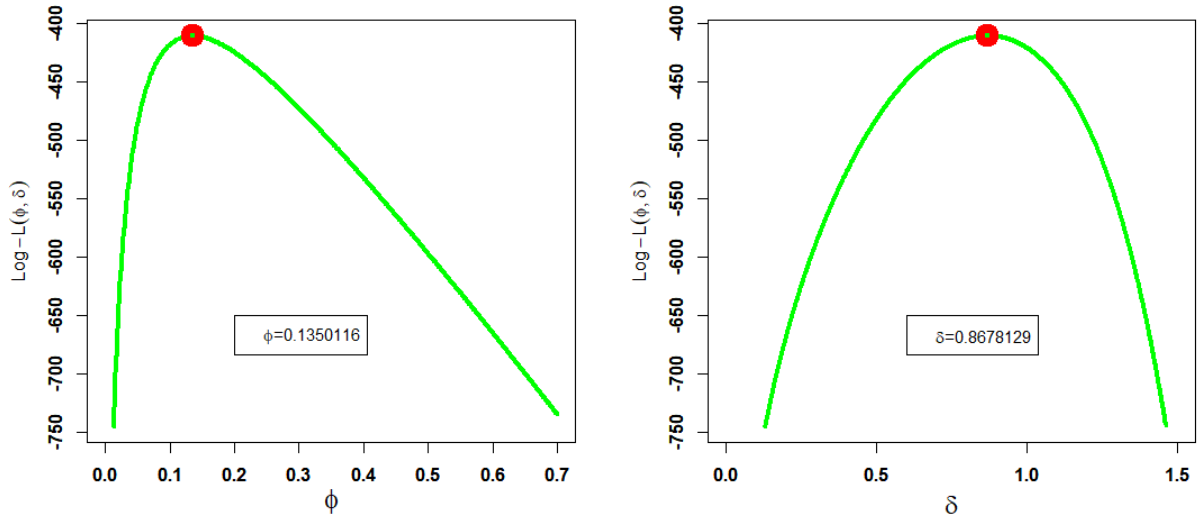

Figure 8. The profile Log-LF plots of the $\hat{\phi}_{MLE}$, and$\hat{\delta}_{MLE}$of the NFLC-Wei distribution for D_1.

Table 5. The values of Δ_1, Δ_2, Δ_3, Δ_4, Δ_5, Δ_6, Δ_7, and P-values of the NFLC-Wei and rival distributions for D_1.

Dist.	Δ_1	Δ_2	Δ_3	Δ_4	Δ_5	Δ_6	Δ_7	**P-Value**
NFLC-Wei	824.9195	830.6235	825.0155	827.2371	0.03568	0.252550	0.036360	0.9968
NRLog-Wei	832.5416	841.0977	832.7351	836.0180	0.06842	0.611860	0.098672	0.5869
Wei	832.1738	837.8778	832.2698	834.4913	0.06996	0.7861914	0.131324	0.5981
APC-Wei	827.1344	835.6905	827.328	830.6108	0.05032	0.3120118	0.052318	0.9021
APT-Wei	826.3801	834.9362	826.5737	829.8565	0.046609	0.2741105	0.042276	0.9437
NEx-Wei	827.5168	833.2208	829.8343	828.6128	0.057143	0.4283166	0.069245	0.7974
NAPT-Wei	826.1121	834.6682	829.5885	828.3056	0.042005	0.2743269	0.031732	0.9776
MO-Wei	829.3199	837.876	832.7963	829.5135	0.054899	0.4320377	0.074033	0.8352

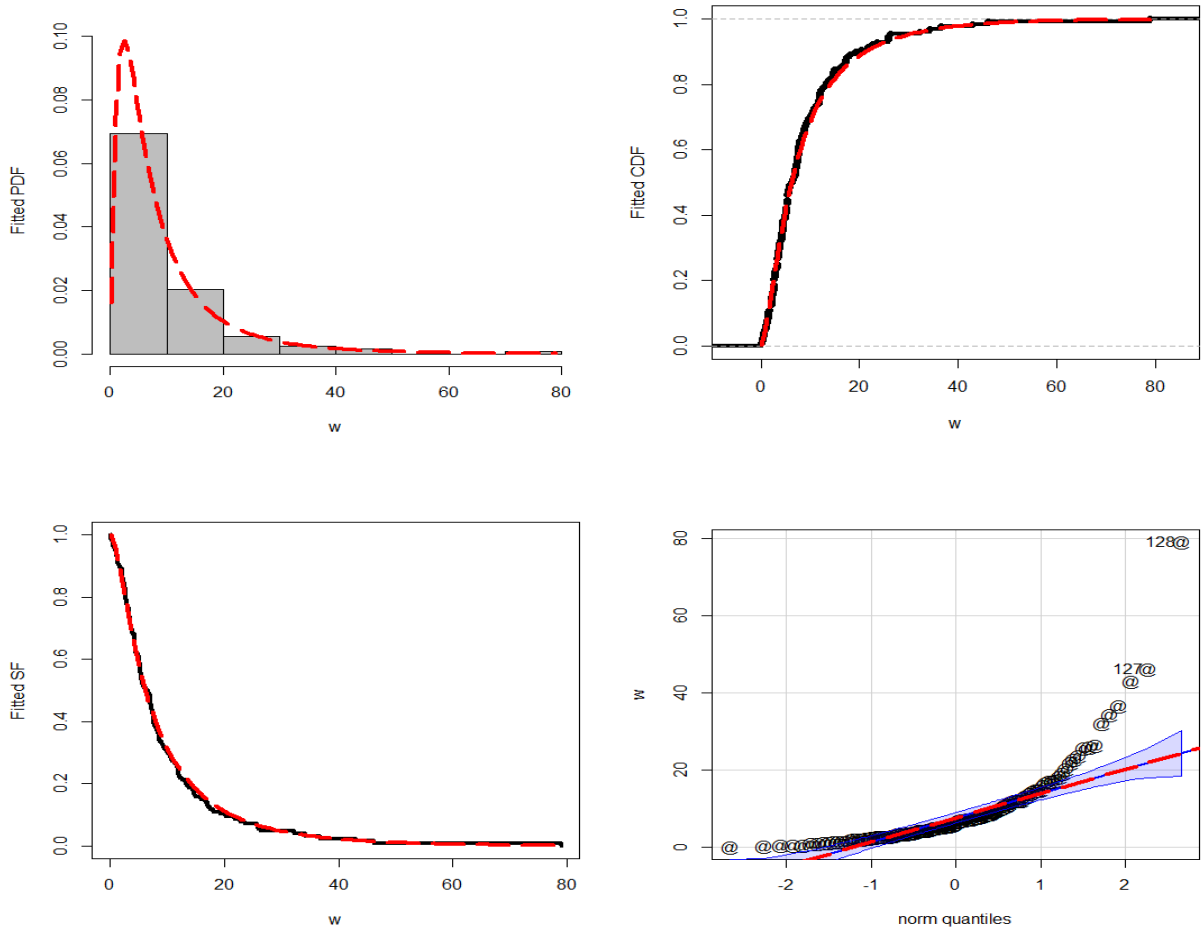

Figure 9. The estimated PDF, CDF, SF, and QQ plots of the NFLC-Wei distribution for D_1

5.3. Analysis of D_2

This part presents the numerical findings of the MLEs and fit quality metrics for the NFLC-Wei and other competing distributions using D_2. The visual representations of the fitting capability of the NFLC-Wei distribution are also depicted usingD_2.

Using D_2, the numerical values of the $\hat{\phi}_{MLE}$,$\hat{\delta}_{MLE}$, and $\hat{\alpha}_{MLE}$of the NFLC-Wei distribution and other competing (or rival) distributions are recorded in Table 6. The profile LLF of the $\hat{\phi}_{MLE}$, and$\hat{\delta}_{MLE}$of the NFLC-Wei distribution is graphically visualized in Figure 10. From Figure 10, we can see that the estimated parameters are unique roots and maximization of the LLF of the NFLC-Wei distribution.

Corresponding to D_2, the numerical descriptions of the goodness of fit measures and p-values of the NFLC-Wei and other competing distributions are recorded in Table 7. From Table 7, for the NFLC-Wei distribution, the goodness of fit measures and P-value are Δ_1 =39.44881, Δ_2 =41.44027, Δ_3 =40.15469, Δ_4 =39.83757, Δ_5 =0.16634, Δ_6 =0.6020544, Δ_7 =0.1004887, and P-value=0.6374. Based on the results of Δ_1, Δ_2, Δ_3, Δ_4, Δ_5, Δ_6, Δ_7, and P-value recorded in Table 7, it is shown that the NFLC-Wei distribution provides the superior and closed fits to the D_2. Because the NFLC-Wei distribution has smaller values of the goodness of fit measures (i.e., Δ_1, Δ_2, Δ_3, Δ_4, Δ_5, Δ_6, and Δ_7) and a higher P-value. Furthermore, based on the results of Δ_1, Δ_2, Δ_3, Δ_4, and Δ_6, the second optimal distribution for theD_2 is the MO-Wei probability distribution. For the MO-Wei distribution, the goodness-of-fit measures are Δ_1 =40.81321, Δ_2 =43.80041, Δ_3 =41.39634, Δ_4 =42.31321, and Δ_6 =0.6689762. Similarly, based on the results of Δ_5, Δ_7, and P-value, the second most valuable distribution for the considered data set is the NAPT-Wei probability distributions because its values Δ_5 =0.17487, Δ_7 =0.1261372, and P-value=0.6109.

After the numerical comparison, we also considered the graphical illustration of the NFLC-Wei distribution by usingD_2. To depict graphically, we illustrated the plots of the estimated PDF, CDF, SF, and QQ plot; refer to Figure 11. The visual representation in Figure 11 further validated that the NFLC-Wei distribution is a more effective distribution for

theD_2.

Table 6. The $\hat{\phi}_{MLE}$,$\hat{\delta}_{MLE}$, and $\hat{\alpha}_{MLE}$ values of the fitted distributions for D_2.

Dist.	$\hat{\phi}_{MLE}$	$\hat{\delta}_{MLE}$	$\hat{\alpha}_{MLE}$
NFLC-Wei	0.14086790	2.55892110	--
FRLog-Wei	0.00448578	4.82780000	0.98623928
Wei	0.12157653	2.78694575	--
APC-Wei	0.01400824	3.45452819	0.01553680
APT-Wei	0.02073824	3.62006739	0.01586639
NEx-Wei	0.04602786	3.32337639	--
NAPT-Wei	0.73428493	1.66463550	55.8836939
MO-Wei	0.00371084	4.40514483	0.04792745

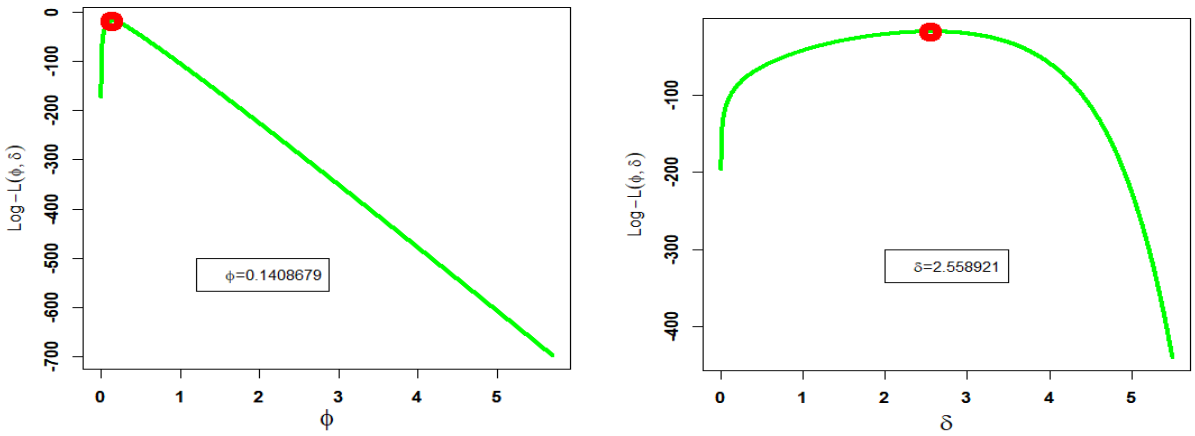

Figure 10. The profile Log-LF plots of the $\hat{\phi}_{MLE}$, and$\hat{\delta}_{MLE}$of the NFLC-Wei distribution for D_2.

Table 7. The values of Δ_1, Δ_2, Δ_3, Δ_4, Δ_5, Δ_6, Δ_7, and P-values of the NFLC-Wei and rival distributions for D_2.

Dist.	Δ_1	Δ_2	Δ_3	Δ_4	Δ_5	Δ_6	Δ_7	**P-Value**
NFLC-Wei	39.44881	41.44027	40.15469	39.83757	0.16634	0.6020544	0.1004887	0.6374
FRLog-Wei	44.70328	47.69047	46.20328	45.28641	0.22294	0.8522219	0.1402434	0.2732
Wei	44.17281	47.16427	45.87869	45.56156	0.18495	1.09287	0.1857121	0.5007
APC-Wei	43.94548	46.93268	45.44548	44.52861	0.18957	0.8242832	0.1405009	0.5985
APT-Wei	43.41718	46.40438	44.91718	44.00031	0.17791	0.7784439	0.1324222	0.6009
NEx-Wei	42.93560	44.92706	43.32435	43.64148	0.18129	0.9042441	0.1521853	0.5267
NAPT-Wei	43.17302	46.16021	43.75615	44.67302	0.17487	0.7466151	0.1261372	0.6109
MO-Wei	40.81321	43.80041	41.39634	42.31321	0.19609	0.6689762	0.1482901	0.5927

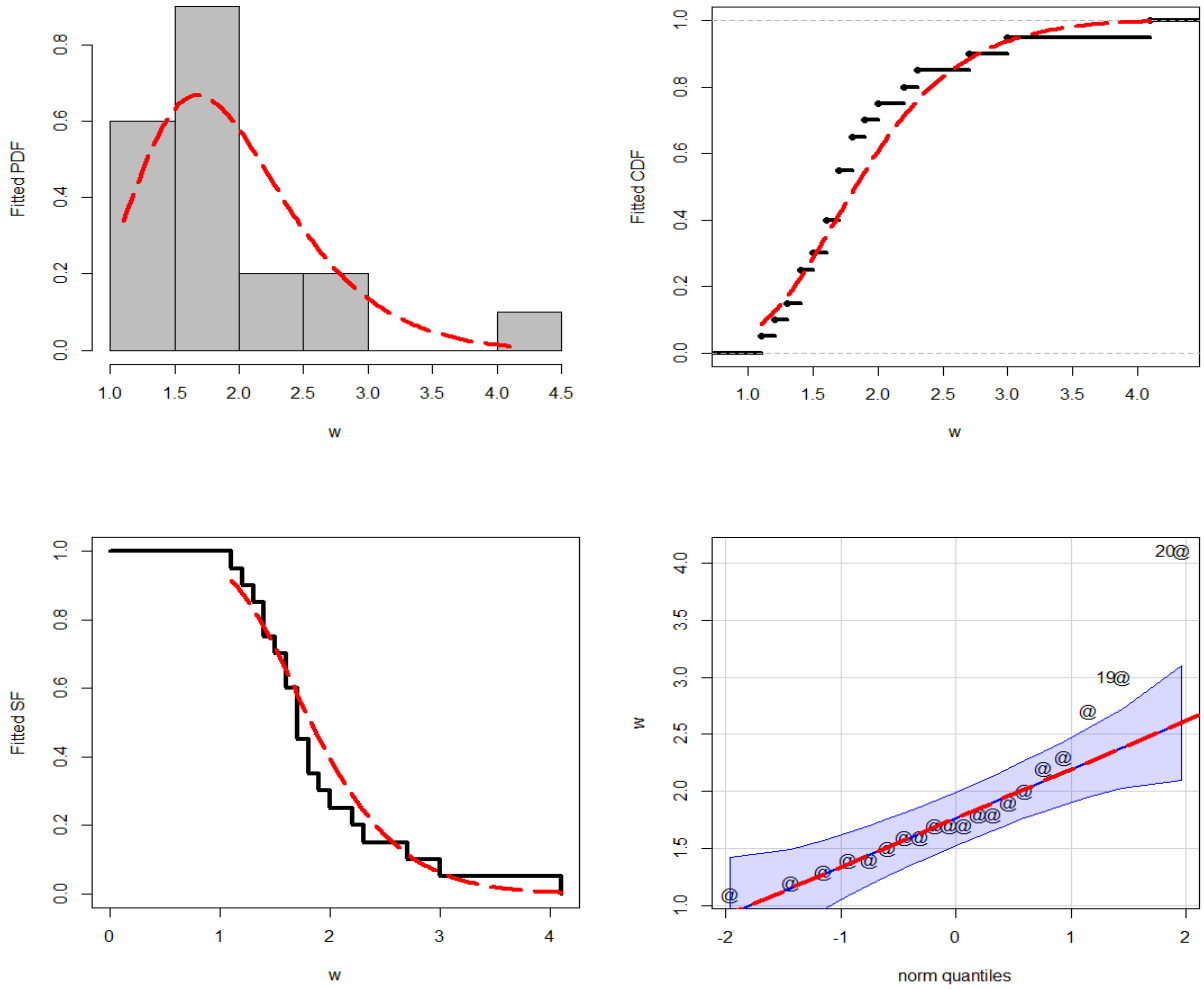

Figure 11. The estimated PDF, CDF, SF, and QQ plots of the NFLC-Wei distribution for D_2.

5.4. Analysis of D_3

In the present sub-part of the article, we present the numerical outcomes of the MLEs and goodness-of-fit statistics for the NFLC-Wei and various competing distributions using D_3. The graphical representations of the fitting capacity of the NFLC-Wei distribution are also depicted by utilizingD_3.

Using D_3, the numerical values of the $\hat{\phi}_{MLE}$,$\hat{\delta}_{MLE}$, and $\hat{\alpha}_{MLE}$of the NFLC-Wei distribution and other competing (or rival) distributions are recorded in Table 8. The profile LLF of the $\hat{\phi}_{MLE}$, and$\hat{\delta}_{MLE}$of the NFLC-Wei distribution is graphically established and illustrated in Figure 12. From Figure 12, we can also see that the estimated parameters are unique roots and maximization of the LLF of the NFLC-Wei distribution.

Corresponding to D_3, the numerical descriptions (evaluation or fitting performance) of the goodness of fit measures and p-values of the NFLC-Wei and other competing distributions are recorded in Table 9. From Table 9, for the NFLC-Wei distribution, the goodness of fit measures and P-value are Δ_1 =560.4502, Δ_2 =564.0186, Δ_3 =560.7429, Δ_4 =561.7736, Δ_5 =0.084285, Δ_6 =0.2482962, Δ_7 =0.0399979, and P-value=0.8874. Based on Δ_1, Δ_2, Δ_3, Δ_4, Δ_5, Δ_6, Δ_7, and the P-value recorded in Table 9, it is observed that the NFLC-Wei distribution provides the superior and closed fits to the D_3. Because in Table 9, the NFLC-Wei distribution has smaller values of the goodness of fit measures (i.e., Δ_1, Δ_2, Δ_3, Δ_4, Δ_5, Δ_6, and Δ_7) and a higher P-value.

Furthermore, based on the results of Δ_1, Δ_3, Δ_4, Δ_5, Δ_6, Δ_7, and the P-value, the second optimal distribution for theD_3 is the NAPT-Wei probability distribution. For the NAPT-Wei distribution, the goodness measures and P-value are Δ_1 =564.2142, Δ_3 =566.1190, Δ_4 =564.8141, and Δ_5 =0.087322, Δ_6 =0.3807588, Δ_7 =0.0623701 and p-value=0.8616.

Similarly, based on the result of Δ_2, the second optimal distribution for the D_3 is the NEx-Wei distribution because its value Δ_2 =569.3743.

After the numerical comparison, we also considered the graphical illustration of the NFLC-Wei distribution by usingD_3. For graphical illustrations, we visualized the plots of the estimated PDF, CDF, SF, and QQ plot, see Figure 13. The visual illustration in Figure 13 also confirmed that the NFLC-Wei distribution is the superior (or best fitted) distribution for the considered data set (i.e., D_3).

Table 8. The $\hat{\phi}_{MLE}$,$\hat{\delta}_{MLE}$, and $\hat{\alpha}_{MLE}$ values of the NFLC-Wei and other rival distributions for D_3.

Dist.	$\widehat{\phi}_{MLE}$	$\widehat{\delta}_{MLE}$	$\widehat{\alpha}_{MLE}$
NFLC-Wei	0.01260272	0.80925010	--
FRLog-Wei	0.02859686	0.76184619	5.72175017
Wei	0.00677126	0.93131153	--
APC-Wei	0.00280928	0.94709838	0.406874901
APT-Wei	0.00326451	0.99270097	0.245030412
NEx-Wei	0.00201269	1.05444359	--
NAPT-Wei	0.17107061	0.51023212	91.1431842
MO-Wei	0.00303242	1.00118851	0.50752438

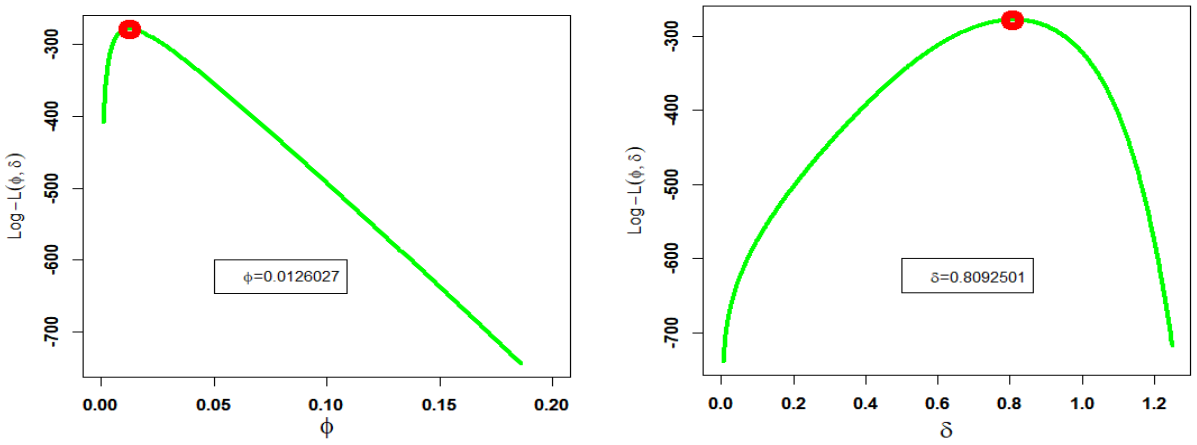

Figure 12. The profile Log-LF plots of the $\hat{\phi}_{MLE}$, and$\hat{\delta}_{MLE}$of the NFLC-Wei distribution forD_3.

Table 9. The values of Δ_1, Δ_2, Δ_3, Δ_4, Δ_5, Δ_6, Δ_7, and P-values of the NFLC-Wei and rival distributions for D_3.

Dist.	Δ_1	Δ_2	Δ_3	Δ_4	Δ_5	Δ_6	Δ_7	P-Value
NLC-Wei	560.4502	564.0186	560.7429	561.7736	0.084285	0.2482962	0.0399979	0.8874
FRL-Wei	572.8833	578.2359	573.4833	574.8683	0.13355	1.0955362	0.1910325	0.3789
Wei	567.6941	571.2625	567.9868	569.0175	0.12612	0.8142793	0.1398362	0.4494
APC-Wei	568.8619	574.2144	569.4619	570.8469	0.10892	0.7171791	0.1223265	0.6340
APT-Wei	567.7712	573.1238	568.3712	569.7562	0.10551	0.5538716	0.0933977	0.6723
NEx-Wei	564.8061	569.3743	566.1293	565.0986	0.10786	0.5356683	0.0900657	0.6459
NAPT-Wei	564.2142	569.5666	566.1190	564.8141	0.087322	0.3807588	0.0623701	0.8616
MO-Wei	568.2084	573.5610	570.1934	568.8084	0.112555	0.561812	0.0949219	0.5933

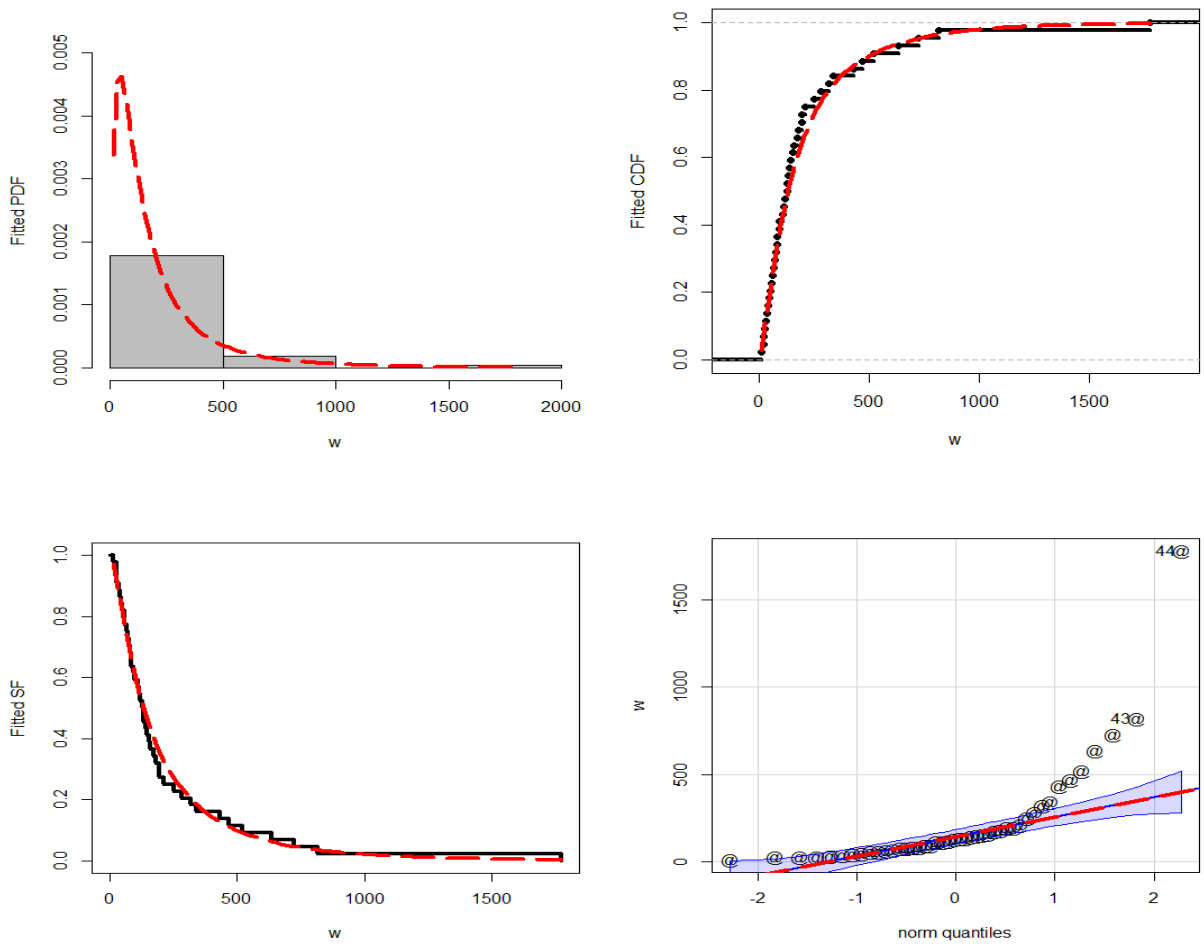

Figure 13. The PDF, CDF, SF, and QQ plots of the NFLC-Wei distribution for D_3.

6. Concluding Remarks

This article proposes a novel approach without introducing any additional parameters by adopting and implementing a novel methodological technique. A Novel Flexible Logarithmic Cosine-G (NFLC-G) family of distributions is the name given to the recently suggested technique. The NFLC-G family of distributions is proposed by implementing the Logarithmic and Cosine functions with the goal of avoiding reparameterization problems. Some fundamental distributional properties of the NFLC-G family are also derived. A special sub-model, Novel Flexible Logarithmic Cosine Weibull (NFLC-Wei) distribution, is developed to illustrate the practical performance of the NFLC-G family of distributions. The model parameters are estimated using the Maximum Likelihood estimation technique. A Monte Carlo simulation analysis is carried out to evaluate the performance of the applied estimation method for the proposed distribution. Additionally, the practicality of the NFLC-G family of distributions is demonstrated by examining three real-world datasets from the biomedical field. The practical performance of the NFLC-Wei distribution is compared using different statistical information criteria with other well-known classical distributions in the literature. Hence, numerically and graphically, it is observed that the NFLC-Wei distribution provides a satisfactory fit to the biomedical datasets. We believe that this newly introduced approach of distributions and its special members can be applied across multiple fields, such as survival analysis, medical research, and reliability engineering, and they may inspire the development of new models in the future.

Authors' Contributions:

Conceptualization, Z.S., Z.A., and G.S.R.; Methodology, Z.S.; Software, Z.S., Z.A, and G.S.R; Formal Analysis, Z.S., Z.A., Z.A., and G.S.R.; Investigation, Z.S., F.K., C.K.O., and S.K.K.; Data Curation, Z.S., Z.A., F.K., C.K.O., G.S.R., and S.K.K.; Validation, F.K., C.K.O., G.S.R., and S.K.K.; Resources, C.K.O., G.S.R., and S.K.K.; Writing –Original Draft

Preparation, Z.S., and Z.A.; Writing –Review & Editing, Z.A., F.K., C.K.O., G.S.R., and S.K.K.; Visualization, Z.S., Z.A., and G.S.R.; Supervision, Z.S., Z.A., and G.S.R.; Project Administration, C.K.O., and G.S.R..

Data Availability Statement:

The data supporting this study's findings are available within the article.

Conflicts of Interest:

The authors declare that they have no conflict of interest.

Funding:

This research received no external funding.

References

1. Yao, M., Zhao, T., Cao, J., & Li, J. (2025). Hierarchical Fuzzy Topological System for High-Dimensional Data Regression Problems. *IEEE Transactions on Fuzzy Systems*, 33(7), 2084-2095.
2. Ren, Y., Zhang, J., Xia, Y., Wang, R., Xie, F., Guan, J., ... & Zhou, S. (2025). Regression-based conditional independence test with adaptive kernels. *Artificial Intelligence*, *347*, 104391.
3. Zhang, X., Zhou, L., Wang, S., Fan, C., & Huang, D. (2025). Facilitating Patient Adoption of Online Medical Advice Through Team-Based Online Consultation. *Journal of Theoretical and Applied Electronic Commerce Research*, 20(3), 231.
4. Jin, J., Chen, W., Ouyang, A., Yu, F., & Liu, H. (2024). A Time-Varying Fuzzy Parameter Zeroing Neural Network for the Synchronization of Chaotic Systems. *IEEE Transactions on Emerging Topics in Computational Intelligence*, 8(1), 364-376.
5. Tian, Z., Lee, A., & Zhou, S. (2024). Adaptive tempered reversible jump algorithm for Bayesian curve fitting. *Inverse Problems*, 40(4), 045024.
6. Gómez, Y. M., Gallardo, D. I., Bourguignon, M., Bertolli, E., & Calsavara, V. F. (2023). A general class of promotion time cure rate models with a new biological interpretation. *Lifetime Data Analysis*, *29*(1), 66-86.
7. Alghamdi, S. M., Shrahili, M., Hassan, A. S., Gemeay, A. M., Elbatal, I., & Elgarhy, M. (2023). Statistical inference of the half logistic modified Kies exponential model with modeling to engineering data. *Symmetry*, *15*(3), 586.
8. Atchadé, M. N., N'bouké, M., Djibril, A. M., Shahzadi, S., Hussam, E., Aldallal, R., ... & El-Bagoury, A. A. H. (2023). A New Power Topp–Leone distribution with applications to engineering and industry data. *PLoS one*, *18*(1), e0278225.
9. Tang, X., Seong, J. T., Alharbi, R., Al Mutairi, A., & Nasr, S. G. (2024). A new probabilistic model: Theory, simulation and applications to sports and failure times data. *Heliyon*, *10*(4), e25651.
10. Sánchez, L., Leiva, V., Saulo, H., Marchant, C., & Sarabia, J. M. (2021). A new quantile regression model and its diagnostic analytics for a Weibull distributed response with applications. *Mathematics*, *9*(21), 2768.
11. AlQdah, K. S., Alahmdi, R., Alansari, A., Almoghamisi, A., Abualkhair, M., & Awais, M. (2021). Potential of wind energy in Medina, Saudi Arabia based on Weibull distribution parameters. *Wind Engineering*, *45*(6), 1652-1661.
12. Sarhan, A. M., & Zaindin, M. (2009). Modified Weibull distribution. *APPS. Applied Sciences*, *11*, 123-136.
13. Rehman, H., Chandra, N., Hosseini-Baharanchi, F. S., Baghestani, A. R., & Pourhoseingholi, M. A. (2022). Cause-specific hazard regression estimation for modified Weibull distribution under a class of non-informative priors. *Journal of Applied Statistics*, *49*(7), 1784-1801.
14. Nofal, Z. M., Afify, A. Z., Yousof, H. M., Granzotto, D. C., & Louzada, F. (2016). Kumaraswamy transmuted exponentiated additive Weibull distribution. *International Journal of Statistics and Probability*, *5*(2), 78-99.
15. Kumar, D., Singh, U., & Singh, S. K. (2015). A new distribution using sine function-its application to bladder cancer patients data. *Journal of Statistics Applications & Probability*, *4*(3), 417.
16. Mahmood, Z., Chesneau, C., & Tahir, M. H. (2019). A new sine-G family of distributions: properties and applications. *Bull. Comput. Appl. Math.*, *7*(1), 53-81.
17. Souza, L., Junior, W., De Brito, C., Chesneau, C., Ferreira, T., & Soares, L. (2019). On the Sin-G class of distributions: theory, model and application. *Journal of Mathematical Modeling*, *7*(3), 357-379.

18. Souza, L., Junior, W. R. D. O., de Brito, C. C. R., Ferreira, T. A., & Soares, L. G. (2019). General properties for the Cos-G class of distributions with applications. *Eurasian Bulletin of Mathematics (ISSN: 2687-5632)*, 63-79.
19. Ampadu, C. B. (2021). The hyperbolic Tan-X family of distributions: Properties, application and characterization. *Journal of Statistical Modelling: Theory and Applications*, *2*(1), 1-13.
20. Eghwerido, J. T., Nzei, L. C., Omotoye, A. E., & Agu, F. I. (2022). The Teissier-G family of distributions: Properties and applications. *Mathematica Slovaca*, *72*(5), 1301-1318.
21. Odhah, O. H., Alshanbari, H. M., Ahmad, Z., Khan, F., & El-Bagoury, A. A. A. H. (2023). A novel probabilistic approach based on trigonometric function: model, theory with practical applications. *Symmetry*, *15*(8), 1528.
22. Ahmad, A., Alsadat, N., Atchade, M. N., ul Ain, S. Q., Gemeay, A. M., Meraou, M. A., ... & Hussam, E. (2023). New hyperbolic sine-generator with an example of Rayleigh distribution: Simulation and data analysis in industry. *Alexandria Engineering Journal*, *73*, 415-426.
23. Sapkota, L. P., Kumar, P., Kumar, V., Tashkandy, Y. A., Bakr, M. E., Balogun, O. S., ... & Gemeay, A. M. (2024). Sine π-power odd-G family of distributions with applications. *Scientific Reports*, *14*(1), 19481.
24. Almetwally, E. M., Hassan, A. S., & Almongy, H. M. (2025). Bayesian Reliability Analysis of a Sine Model Under Hybrid Censoring. *IEEE Access,* 13, 166397-166418.
25. Jiang, L., Seong, J. T., Alhelali, M. H., Alsaedi, B. S., Alghamdi, F. M., & Aldallal, R. (2024). A new cosine-based approach for modeling the time-to-event phenomena in sports and engineering sectors. *Alexandria Engineering Journal*, *98*, 19-31.
26. Odhah, O. H., Alshanbari, H. M., Ahmad, Z., & Rao, G. S. (2023). A weighted cosine-G family of distributions: properties and illustration using time-to-event data. *Axioms*, *12*(9), 849.
27. Shah, Z., Ali, A., Hamraz, M., Khan, D. M., Khan, Z., El-Morshedy, M., ... & Almaspoor, Z. (2022). A New Member of T-X Family with Applications in Different Sectors. *Journal of Mathematics*, *2022*(1), 1453451.
28. Weibull, W. (1951). A statistical distribution function of wide applicability. *Journal of Applied Mechanics.*
29. Alghamdi, A. S., & Abd El-Raouf, M. M. (2023). A New Alpha Power Cosine-Weibull Model with Applications to Hydrological and Engineering Data. *Mathematics*, *11*(3), 673.
30. Dey, S., Sharma, V. K., & Mesfioui, M. (2017). A new extension of Weibull distribution with application to lifetime data. *Annals of Data Science*, *4*, 31-61.
31. Elbatal, I., Ahmad, Z., Elgarhy, M., & Almarashi, A. M. (2018). A new alpha power transformed family of distributions: properties and applications to the Weibull model. *Journal of Nonlinear Science and Applications*, *12*(1), 1-20.
32. Marshall, A. W., & Olkin, I. (1997). A new method for adding a parameter to a family of distributions with application to the exponential and Weibull families. *Biometrika*, *84*(3), 641-652.
33. Liu, Y., Ilyas, M., Khosa, S. K., Muhmoudi, E., Ahmad, Z., Khan, D. M., & Hamedani, G. G. (2020). A Flexible Reduced Logarithmic-X Family of Distributions with Biomedical Analysis. *Computational and Mathematical Methods in Medicine*, *2020*(1), 4373595.
34. Lee, E. T., & Wang, J. (2003). *Statistical methods for survival data analysis* (Vol. 476). John Wiley & Sons.
35. Shah, Z., Khan, D. M., Khan, I., Hussain, S., Alghamdi, F. M., & Aljohani, H. M. (2025). A new flexible odd type-G family of distributions with properties and applications in the biomedical sector. *Scientific Reports*, *15*(1), 35490.
36. Shah, Z., Khan, D. M., Khan, Z., Faiz, N., Hussain, S., Anwar, A., ... & Kim, K. I. (2023). A new generalized logarithmic-X family of distributions with biomedical data analysis. *Applied Sciences*, *13*(6), 3668.
37. Odhah, O. H., Alshanbari, H. M., Ahmad, Z., Khan, F., & El-Bagoury, A. A. A. H. (2024). A new family of distributions using a trigonometric function: Properties and applications in the healthcare sector. *Heliyon*, *10*(9).